2018

Evidence for extra-gastric expression of the proton pump H+/K+ -ATPase in the gills and kidney of the teleost Oreochromis niloticus

Ebtesam Barnawi
barn9740@mylaurier.ca

Evidence for extra-gastric expression of the proton pump H^+/K^+ -ATPase in the gills and kidney of the teleost *Oreochromis niloticus*

Ebtesam Ali Barnawi

Bachelor of Science, Zoology, King Abdul-Aziz University 2012

Thesis

Submitted to the Department of Biology

Faculty of Science

In partial fulfillment of the requirements for the

Master of Science in Integrative Biology

Wilfrid Laurier University, Waterloo, Ontario Canada

2017

Abstract:

It is well known that stomach acid secretion by oxynticopeptic cells of the gastric mucosa is accomplished by the H^+/ K^+-ATPase (HKA), which is comprised of the HKα1 (gene: *atp4a*) and HKβ (gene: *atp4b*) subunits. However, the role of the HKA in extra-gastric organs such as the gill and kidney is less clear especially in fishes. This pump may contribute to active ion and/or acid-base regulation either through direct ion transport or through secondary transport proteins against unfavorable electrochemical gradients via the energy derived from ATP hydrolysis. In the present work I have demonstrated uptake of the K^+ surrogate flux marker rubidium (Rb^+) *in vivo* in *O. niloticus*; however, this uptake was not inhibited with omeprazole, a potent inhibitor of the gastric HKA. This contrasts with gill and kidney *ex vivo* preparations where tissue Rb^+ uptake was significantly inhibited by omeprazole and SCH28080, another gastric HKA inhibitor. To determine the cellular localization site of this pump in both gills and kidney I used immunohistochemical techniques using custom made antibodies specific for Atp4a and Atp4b. Antibodies against both subunits showed the same apical ionocyte distribution pattern in gill and collecting tubules in kidney. Taken together these results indicate for the first time K^+ (Rb^+) uptake in *O. niloticus* and that the HKA can be implicated by the *ex vivo* uptake inhibition by omeprazole and SCH28080, verifying a role for HKA in K^+ absorption in the gill's ionocytes and collecting tubule segment of the kidney.

Acknowledgements

I wish to thank my supervisor Dr. Jonathan M. Wilson for giving me the opportunity to pursue this degree and being very patient, and welcoming me and all my questions and concerns every time I needed him. Heartfelt thanks for him for teaching me step by step and advising me through my research.

I wish to also thank Dr. James C. McGeer and Dr. Michael P. Wilkie as my committee members, for their feedbacks which improved my work. I would like to acknowledge Afshan Ardalan for helping me with many biochemistry mechanisms. My thanks is extended to the NSERC for the financial support to Dr.Wilson and Saudi Arabian Cultural Bureau, for supporting me and my research providing all financial expenses all the way through my scholarship.

Regardless of the distance, many thanks to my parents and sisters for staying with me and giving me the love, strength and support to achieve my goal.

Table of content

CHAPTER 2: Materials and Methods

List of Tables

List of figures

ABBREVIATION

APS	amino-propylsilane
$CaCl_2$	Calcium chloride
CsCl	Cesium chloride
D.sabina	*Dasyatis sabina*
DMSO	Dimethyl sulfoxide
FASC	formic acid and sodium chloride
FSM	Fish skin gelatin
gHKA	gastric H^+/K^+-ATPase
HKA	H^+/K^+-ATPase
HNO_3	Nitric acid
K^+	Potassium ion
KCl	Potassium chloride
KH_2PO_4	Mono-potassium phosphate
K_m	Michaelis-Menten constant
$MgSO_4$	Magnesium sulfate

MS222	Tricaine-methane sulfonate
Na^+	Sodium ion
NaCl	Sodium chloride
NADH	Lactate dehydrogenase
NaH_2PO_4	Mono-sodium phosphate
$NaHCO^-_3$	Sodium bicarbonate
NBF	Neutral buffered formalin
NKA	Na^+/K^+-ATPase
Omz	Omeprazole
PB	Phosphate buffer
PBS	Phosphate buffered saline
Rb^+	Rubidium ion
RbCl	Rubidium chloride
TCA	Trichloro-acetic acid
Vmax	Maximum rate of enzyme reaction

CHAPTER 1

GENERAL INTRODUCTION

1.1 Teleost Osmoregulation

Studies in teleost fishes are important to gain a better understanding of ionic uptake and/or acid-base regulatory mechanisms in both sea water (SW) and fresh water (FW). Many applications and studies of advanced cellular, molecular, and physiological approaches on osmoregulatory organs such as gill have been conducted. They have addressed the morphology of ionocytes (apical structure and cellular ultrastructure), and flux mechanisms necessary to maintain the internal homeostasis to cope with changing aquatic environments including; temperature, pH, ion levels, and salinity (Evans et al. 2005; Hwang et al., 2011).

In the aquatic environment, fishes are exposed to many challenges that require regulation of ions and acid-base balance between the internal and external surroundings (Perry & Gilmour, 2006). Fishes' necessity to maintain homeostasis of intracellular and extracellular pH, have been studied *in vivo* for over 70 years and are well characterized in a number of species (Evans 2008). Studies have investigated the strategies that fishes utilize primarily by their gills, which are the major site of ion and acid-base transfers with the water to maintain homeostasis (Evans et al. 2005). Fishes utilize physiological systems that are responsible for regulation of acid and/or base relevant substances and are designed for buffering and excretion to defend against intracellular and extracellular pH changes (Marshall and Grosell 2006).

Evans (2002) further emphasizes the regulatory mechanisms used in SW teleost fishes, that pump out the excess of absorbed ions via the mitochondrion-rich cells [chloride cells (CC) or ionocytes]. These CCs are localized in both the gill lamellae and filaments of teleost fishes (Wilson and Laurent 2002). As marine fishes consume large quantities of seawater in order to compensate for osmotic dehydration they actively excrete Na^+ and Cl^- via CCs (Evans et al. 2005). In contrast,

FW fishes compensate for the diffusive loss of ions by active uptake of Na^+ and Cl^- driven by active pumps (Evans et al. 2005). They also maintain water homeostasis by excreting dilute urine to the environment (Fig. 1.1) (Marshall and Grosell 2006). Na^+ and Cl^- are the main ions involved in active ion regulation and are linked to acid-base regulation through exchange with the acid and base equivalents H^+ and HCO_3^-, respectively. It is important to note that these exchanges would serve a dual role in acid base and ion regulation in fresh water fishes. However, in seawater the uptake of Na^+ and Cl^- would exacerbate the salt load faced by the fish (Evans, 2002). Marshall and Grosell (2006) advocate this view suggesting that fishes enhance their acid-base secretory capacity to restore body fluid acid-base homeostasis at the cost of an additional ion load.

In FW teleost fishes, acid-base transport across the gill epithelium via an apical exchanger mechanisms located in the outer membrane of the chloride cells (CCs) and possibly in pavement or respiratory cells (PVCs) (Evans et al., 2005). As mentioned above, these cells are the major cells that actively transport ions and maintain ion homeostasis in body fluid. Consequently, these gill cells play a role in the ion osmoregulatory mechanisms along with the kidneys, and intestine (Hwang et al., 2011; Marshall and Grosell 2006). Further the branchial epithelium is fundamentally responsible for the majority of acid base movements (90% or higher) and is a unique organ for aquatic animals followed by kidney and bladder (Perry & Gilmour 2006).

1.1.1 Gills:

The gills are composed of a series of arches that provide the physical support for the gill filaments, which are also called primary lamellae. Each gill arch is supported by calcified vertical elements of the cartilaginous branchial skeleton rays that joined with muscles (Wilson & Laurent, 2002). The gill is well vascularized and brings the fishes' blood close to the aquatic environment

making it the primary site of aquatic respiration and gas exchange (oxygen and carbon dioxide). It also appropriately regulates the correct acid-base balance and metabolic waste (ammonia) excretion (Goss et al.1998; Evans et al. 2005; Hwang 2011). According to Wilson and Laurent (2002), there are two cell types that are potentially involved in gill ionic uptake: pavement cells (PVCs), and mitochondrion-rich cells (MRCs), which is supported by others (Perry et al., 2003; Evans et al. 2005; Shin et al. 2009). The gill epithelium is primarily composed of PVCs covering the gill lamellae (>90% of the surface area) and a few other distinct cell types, such as MRCs that are typically found in the filament epithelium. PVCs are important sites for gas exchange because they are flattened cells with an extensive apical surface area. However, Evans et al. (2005) have also suggested that some PVCs may play an active role in ion and acid-base transport by the gill, and it has been demonstrated that a vacuolar-type proton-ATPase, which participates in acid secretion, is present in the gill epithelium (Evans et al. 2005; Hwang et al., 2011).

Lin & Randall (1991) provided the first evidence of this using trout gill homogenates to demonstrate that the fish gill has a vacuolar-type proton pump (H^+-ATPase) in the epithelium, and that it is involved in H^+ excretion. Then Choe et al. (2004) showed that there is some evidence of a role of H^+/K^+-ATPase in acid-base regulation in an elasmobranch fish gills.

1.1.2 Kidney:

The teleost kidney is a collection of renal tubules (nephrons) that have glomeruli. Each glomerular nephron consists of a renal corpuscle containing the glomerulus and a neck segment followed by two or three proximal segments that connect directly to the collecting duct through the collecting tubule which makes up the major portion of the nephron (Marshall & Grosell, 2005). Perry et al. (2003) have indicated that the kidney has an essential role in controlling HCO_3^- in the

filtrate, therefore, suggesting that it is not less important than the gill in overall acid and/or base excretion and regulating systemic acid base balance. Although, it is not disputed that nitrogenous waste is excreted mainly across the gills, primarily as ammonia, in the kidney there is an exchange for a needed ion (Marshall & Grosell, 2005). Perry et al. (2003) and Koeppen (2009) have further determined that the cells of the nephron secrete H^+ into the tubular fluid and reabsorb the filtered load of HCO_3^-, so approximately 80% of this filtered load is reabsorbed by the proximal tubule, and 16% is reabsorbed by the thick ascending limb and distal tubule, the rest (4%) is reabsorbed by the collecting duct. The mechanism for apical H^+ secretion is maintained by a vacuolar H^+-ATPase that is responsible for approximately one third of HCO_3^- reabsorption, by secreting H^+ into the tubular fluid across the apical membrane, whereas the HCO_3^- exits the cell across the basolateral membrane of the collecting duct while the tubular fluid is acidified.

Collecting duct and intercalated cells have a crtitical role in regulating local and systemic acid-base balance between the plasma membrane and cytoplasmic vesicles (Brown & Bouley, 1998). Intercalated cells are the kidney's mediators of urine acidification, proton secretion and systemic acid-base balance (Brown & Bouley, 1998). According to Caplan (1998), H^+/K^+ -ATPase is certainly also involved in extra gastric roles such as in renal acid-base regulation in tetrapod including mammals. Welling (2013) and Gumz et al. (2010) additionally summarized that kidney H^+/K^+ -ATPase has an established role in potassium and acid-base regulation**,** which controls potassium absorption, and could potentially contribute for efficient renal potassium excretion.

1.2 Potassium and acid-base regulation:

Most ion and/or acid-base regulation in (FW) and (SW) teleost studies were focused on Na^+, Cl^- and Ca^+ ions, and since, K^+ and Na^+ maintain the normal osmotic pressure in most cells,

K^+ is an ion of interest, as it is an essential and natural element that plays a critical role in nerve, muscle and many other vital cell functions, such as metabolism, growth, and repair (Talling, 2010). Talling (201) further explains the position of K^+ in regulating the acid–base balance in the body when exchanges with the outer medium providing biological rhythms. In addition, K^+ affects the kidney's ability to reabsorb bicarbonate as the main extracellular buffer to metabolic acids. Studies by Eddy (1975) and Gairdaire et al. (1991,1992) suggest the possibility of branchial uptake of K^+ from the water in rainbow trout, although, the mechanism remains unknown.

1.3 H^+/K^+-ATPase:

According to Welling (2013) the proton/ potassium adenosine triphosphates, H^+/K^+-ATPase, leads the sustainable balance between the excretion of K^+ and dietary intake, that when K^+ intake is normal or increased, K^+ is secreted, whereas when K^+ dietary is limited, the secretory activity reduces and enhanced activity of the H^+/K^+-ATPase and increases K^+ reabsorption. The H^+/K^+-ATPase participates in K^+ absorption and H^+ secretion, using the energy derived from the hydrolysis of ATP to pump hydrogen H^+ and K^+ ions against their concentration gradients (Shin et al. 2009) (Fig. 1.4).

This enzyme pumps ions through a series of conformational changes from an E1 (ion site in) to an E2 (ion site out) (Shin et al., 2009). The ion exchange process includes a series of catalytic intermediates termed E1, E1P, E2P, and E2, with P denoting a phosphorylated intermediate (Ekberg et al., 2010). These enzymes have been classifies as type II, P-type ATPases since they form high energy phosphorylated intermediate during the catalytic cycle (Pedersen & Carafoli 1987). The H^+/K^+-ATPase is comprised of a HKα1 (gene: *ATP4A*) and HKβ (*ATP4B*) subunits (Fig. 1.2). The β-subunit is unique to the gastric H^+/K^+-ATPase and is thought to be involved in

stabilizing cellular targeting of the transporter. The α-subunit catalyzes ATP hydrolysis and ion translocation and contains 1,035 amino acids. It is the main focus in this research because it is the one responsible in transporting charged substrates across membranes actively. Additionally, it belongs to the large subgroup of the family (type IIc) that includes the gastric H^+/K^+-ATPase (HKα1), non-gastric /colonic H^+/K^+-ATPase (HKα2) and Na^+/K^+-ATPases (NKα). (Choe, Verlander, Wingo, & Evans, 2004)

1.3.1 Gastric H^+/K^+-ATPase

According to Shin et al., (2009), the gastric H^+/K^+-ATPase, is the integral membrane protein responsible for gastric acid secretion. This enzyme appears in cytoplasmic membrane tubules and vesicles in the resting state and then in the expanded secretory canaliculus of the parietal (acid secreting) cells in the stimulated state, once the enzyme moves to the canaliculus, the enzyme secrets acid by the exchange of cytoplasmic H^+ with extracellular K^+.

The gHK-ATPase is the proton pump of the stomach that transport acid against the body's largest concentration gradient, and produces the gastric acid (HCl) as a digestive fluid, with a pH between 1.5 and 3.5 which is secreted with pepsinogen from chief cells to achieve acid-peptic digestion. (Singh et al. 2013; Wilson & Castro 2010; Caplan, 1998). The stoichiometry of gHK-ATPase is 2H/2K/ATP at pH 6.1 that falls to 1H/1K/ ATP as luminal pH falls to <3.0, (Shin, et.al,2009)

Shin et al. (2009) further asserts that there are K^+ efflux channels essential for gastric acid secretion, KCNQ1 and KCNE2. These channels were the most highly expressed and significantly efficient among the large variety of K^+ channels expressed in the gastric epithelium. Codina &

DuBose (2006) demonstrated the function of these channel in supplying K^+ to the luminal surface of the pump in the first place to allow H^+ for K^+ exchange using specific KCNQ inhibitors.

1.3.2 Proton pump inhibitor (PPI)

Firstly, in order to control and activate this pump, changes in locations are required from cytoplasmic vesicles and tubules into the microvilli of the secretory canaliculus of the parietal cells (Singh et al., 2013), as, this enzyme appears to be in the resting state E_1 in cytoplasmic tubular membranes and then in the microvilli of the expanded secretory canaliculus in the stimulated state E_2 of the parietal cell (Shin et al., 2009). However, there are unique drugs that inhibit specific enzymatic activity called proton pump inhibitors (PPIs), and acid pump antagonists (APAs), which are both now the mainstay of treatments of all acid related diseases. Codina & DuBose (2006) made comparisons between these class of drugs and their inhibition efficiencies. Shin et al. (2009) have advocated the view that acid secretion is inhibited by these drugs. PPIs, are developed to block the enzyme activity, and inhibit about 70% of the pump enzyme, owing to their short half-life as not all pump enzymes are activated. Omeprazole was the first drug of PPIs class to be introduced into clinical use in 1989. It inhibits the gHK-ATPase by covalent binding, hence, the duration of its effect is longer than expected from their levels in the blood. In contrast APAs developed for control of acid secretions do not require secretion to inhibit the enzyme activity. Unlike omeprazole, SCH28080 was expected to be fast and effective, as it provided very high affinity to the H^+/K^+-ATPase with excellent inhibition and do not require acid activation which is necessary for PPI activation.

1.3.3 HKA binding mechanism with K^+ (Rb^+) and PPIs:

The P-type ATPase family have four dimensional sites that are involved in the basic ion exchange mechanisms including: a nucleotide-binding domain (N), a phosphorylation domain (P), an actuator domain (A), and a transmembrane domain (M) (Fig 1.4). These four domains are responsible for ATP hydrolysis, and are coupled to ion exchange through the opening and closing of transport pathways that lead to the ion binding site since the coordinating P-domain is highly observed as a K^+ binding site among all P-type ATPases.

The E1 form of the enzyme with high affinity for K^+ allows access to the ion binding domain from the cytoplasmic surface and following binding of ATP with two K^+ ions, then the conformation change from the E1 form to the E1.P conformer where the P domain bends and the hydronium ions bind. This is followed by conversion to the E2.P rotation form where the proton is released outward, the P-domain unbends and, K^+ binds from the luminal surface through K^+ channels. ATP phosphorylates the enzyme and promotes the E2 at this point the stoichiometry of protons extruded per ATP binding, allows acid stable phosphorylation and binding of APAs or PPIs. While PPIs are inactive drugs in their native form when acid is transported by the ATPase, the second proton is added, and then the compound can be activated. However, all PPIs binds to the enzyme in the E2 configuration. On the other hand the APAs, including, SCH28080, bind selectively to the E2P or E2 form of the enzyme (Shin et al., 2009).

1.3.4 Extra-gastric H^+/K^+-ATPase:

It is well known that in mammals, the stomach is the primary organ for acid secretion that is mediated by the gHK-ATPase, followed by the kidneys which is important for acid-base and K^+

regulation. Elasmobranchs also secrete acid from their stomachs by the oxynticopeptic cells in the gastric glands of the mucosa, but unlike mammals they primarily use their gills for systemic acid excretion instead of their kidneys (Choe et al., 2004; Liquori et al., 2005). However, the presence of the extra gastric H^+/K^+-ATPase proton pumps (outside the stomach) remain debatable, conflicting, or unsolved, due to differences in species and experimental designs, as well as limitations of methodologies (Evans et al. 2005).

An extra-gastric role of H^+/K^+-ATPase in the kidney was first established in tetrapod as reviewed by Gumz et al. (2010). A study conducted in the outer medullary collecting ducts (OMCD) of rabbits maintained on low K^+ diets suggests that gHK-ATPase acidifies the tubular fluid and reabsorbs K^+ in the kidney, where it is thought to function in systemic ion and/or acid base regulation (Gumz et al., 2010). In elasmobranchs, gills have many of the functions of kidneys in mammals, for instance, the gills of elasmobranchs are responsible for 90 –100% of systemic net acid excretion during acidosis and are the site of active K^+ absorption in fresh water. With this in mind, another extra-gastric role of H^+/K^+-ATPase was observed in elasmobranchs (Atlantic stingray*, Dasyatis Sabina*) by Choe et al. (2004). This was the first study to demonstrate the expression of gHK-ATPase in the gills by detecting low expression level of HKα1 in the gills by immunohistochemistry and immunoblotting that is similar to that of mammalian gastric parietal cells and renal intercalated cells. HKα1 staining was located in the gastric glands and in the NKA–rich gill epithelial cells where it may function in K^+ absorption.

1.3.5 Rubidium as a substitute for Potassium

Rubidium offers several advantages that makes it a suitable replacement for potassium for flux studies. Rubidium has similar physicochemical behaviors and characteristics to those of

potassium. For instance, both are alkali metals and their hydration radii are similar. Also Rb^+ at high concentrations of exposure has limited toxicity comparable to potassium with the same concentration that would kill the organism. In the environment and in the body Rb^+ represents at very low concentrations, therefore, accumulation within the organism during flux studies is indicative of uptake from the water during exposure(Dietz and Byrne, 1990) (Sanders and Kirschner, 1983; Tipsmark and Madsen, 2001; Mähler and Persson, 2012; Wilcox and Dietz, 1995).

1.3.6 Immunohistochemistry for transporter localization

Immunocytochemistry (IHC) is one of the most productive techniques in research which is used to identify the location of proteins in tissues and cells (Harlow & Lane 1988). There are three combinations required for effective and accurate IHC labeling using an indirect technique. These include specific primary antibodies, marker conjugated species specific secondary antibodies and negative control serum. The IHC methods used in this thesis was co-localization or double-labeling methods to detect two different antigens in the same tissue section. Hence, two different primary antibodies to different epitopes on the same antigen overlap to confirm the primary antibody is specific for the protein (Burry, 2011; Harlow & Lane, 1988)

Antibodies have been used as powerful probes that are responsible for many significant discoveries to localize structures in tissue sections. The structure of the antibody contains a variable region (Fab portion) which binds the epitope part of the antigen, and the constant region (the Fc portion) is specific to the animal where the antibody was raised. The primary antibody is the antibody specific of the antigen of interest binding to the correct epitope on the expected antigen. The secondary antibody, is the antibody that binds the Fc portion of the primary antibody,

in a species-specific manner and has a marker molecule conjugated to it for visualization in sections. These markers can be enzymes (e.g. horse radish peroxidase or alkaline phosphatase), gold particles or fluorophores (e.g. Alexa dyes). Negative control samples are required to show that the label localization is correct and accurate (Burry, 2011).

The antibodies used in this research were as follow: The monoclonal α5 antibody, which was developed by Dr. Fambrough, Johns Hopkins University, and was obtained from the Developmental Hybridoma Bank in the University of Iowa, Iowa City. It binds to all isoforms and types of NKA and is been used widely to recognize fish NKA (Wilson & Laurent 2002). In the thesis, this antibody was used as a marker for gill ionocytes (Wilson & Laurent 2002). The custom polyclonal primary HKA antibodies Atp4a-B1351 and B1352 and Atp4b-B1349 and B1350 were produced in chicken using synthetic peptides of Atp4a and Atp4b and isolated as chicken egg yolk immunoglobulin G **(**IgY) obtained from Genetel Inc (USA). The polyclonal secondary antibodies used were goat anti-mouse IgG conjugated to the fluorophore Alexa 555 (Abcam, UK) and goat anti-chicken IgY conjugated to either CF640 (Biotium, USA) or Alexa 488 (Abcam).

1.4 Species selection:

The species name of the Nile tilapia has changed over time. During 1970s the Nile tilapia was initially described as *Tilapia nilotica*, then became *Sarotherodon niloticus* and is now called *Oreochromis niloticus* (*O. niloticus*). The last revision has now been widely accepted in the scientific literature. Nile tilapia is most importantly a hardy species. They can be euryhaline (tolerate a wide range of salinity levels) or inhabit varied freshwater habitats, in addition to their aquaculture availability. It is widely accepted that *O. niloticus* is one of the best species for warm water aquaculture since it is an omnivorous feeder that can filter feed on plankton as well as

accepting larger food particles (Arrignon, et al.,1998). This species is also relatively robust and disease free, and is capable of rapid growth. The male fish grows faster and to a greater size than the female, and they both become sexually mature at 6-7 months after hatch (Maclean et al., 2002).

O. niloticus is also a well-studied species for fish biology. Therefore, it was chosen as a model species of significance as its genome has been sequenced and annotated (ensemble.org). Lower vertebrates potentially express three HKα isoforms: HKα1 (*atp4a*), HKα1b (*atp4a2*), and HKα 2 (*atp12a*) to facilitate K^+ uptake and H^+ excretion. However, Nile tilapia lacks the *atp12a* gene. The *O. niloticus* genome also only has one HKα1 gene, which will simplify the analysis of results. (J.M. Wilson unpublished) (Fig. 1.3).

1.5 Aim of Thesis

The role and expression of the gastric proton pump H^+/ K^+-ATPase in teleost fishes remains unsolved or unclear due to variances in species and experimental strategies, in addition to the limitation of methodologies. This thesis will provide the first evidence for the expression of gastric proton pump H^+/ K^+-ATPase - (gene: *atp4a and atp4b*) in a teleost fish and demonstrate its potential role in potassium and acid base regulation. Consequently, the central ***objective:*** of this thesis is to investigate the role of this pump in extra-gastric potassium and acid-base regulation in the gill and kidney of the teleost fish *O. niloticus*. Several experimental observations supported the ***hypothesis*** that the gastric proton pump H^+/ K^+-ATPase has a role in active K^+ absorption in gill and kidney, and that it is expressed in the ionocytes of the gill and the intercalated cells of the kidney collecting duct, where it is involved in branchial and renal potassium and acid-base regulation, respectively.

Rb^+ was used as a surrogate flux marker for K^+ and two experimental approaches were taken which included: an *in vivo* and *ex vivo* Rb^+ uptake assays to analyze the H^+/ K^+-ATPase activity in gill and kidney. To better determine if the H^+/ K^+-ATPase was specifically involved in Rb^+ uptake, a pharmacological inhibition assays of Rb^+ uptake and H^+ excretion with the gastric H^+/ K^+-ATPase inhibitors SCH28080 and omeprazole were performed. In addition, a tissue viability assay was performed using *ex vivo* preparations. Specifically, the lactate dehydrogenase (LDH) assay was used as an indicator or cell damage by measuring activity of this enzyme in the culture medium leaked from damaged cells. Finally, the expression of Atp4a and Atp4b in the gill and kidney was established using immunohistochemistry (IHC) with custom made antibodies to identify the presence and subcellular location of these subunit proteins within these tissues.

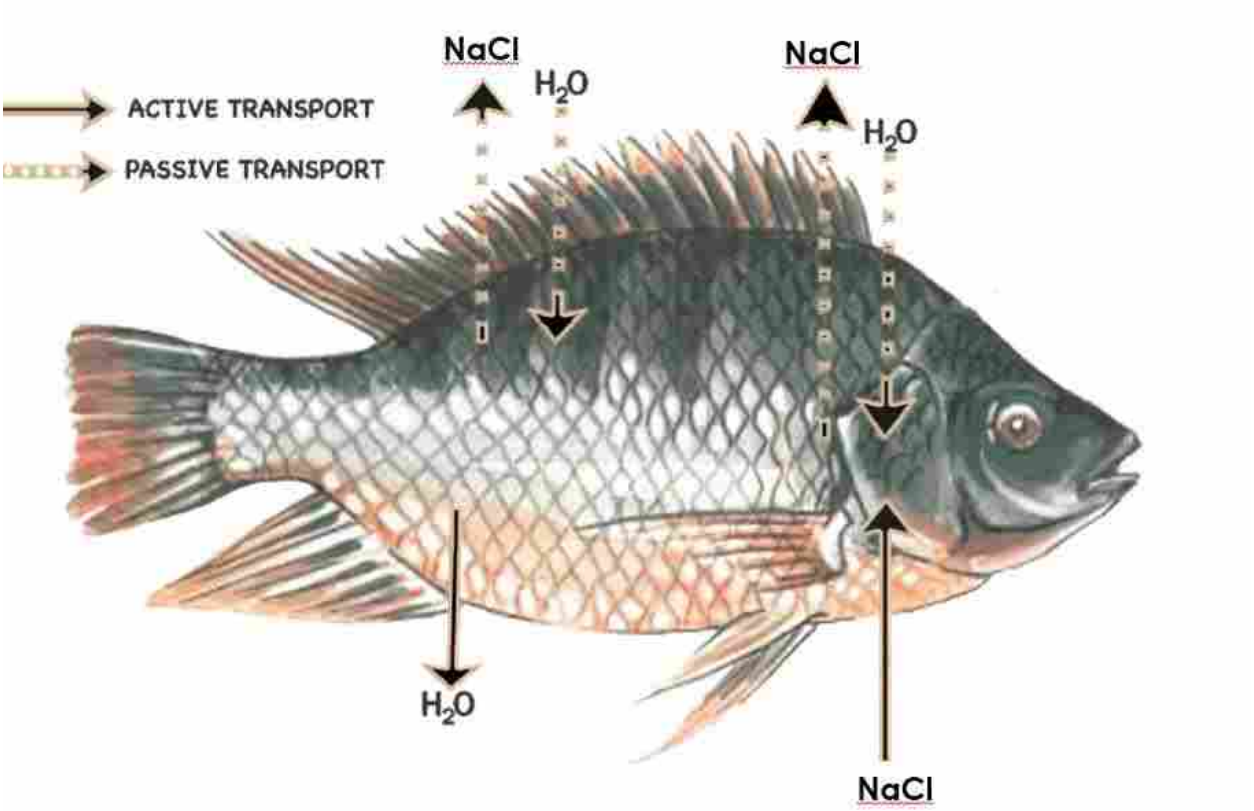

Figure 1.1. The mechanisms of osmoregulation for freshwater fishes. Solid arrows represent the active transport of ions and water, whereas the dash arrows show the passive diffusion of ions and water across the fish. *Oreochromis niloticus* loses ions and gains water across the gills and skin. They compensate for the passive loss of ions by active uptake of Na^+ and Cl^- (and K^+) at the gills from low concentrations in the water again higher internal concentrations using ATP hydrolysis and get rid of excess water through their kidney by excreting abundant amount of dilute urine.

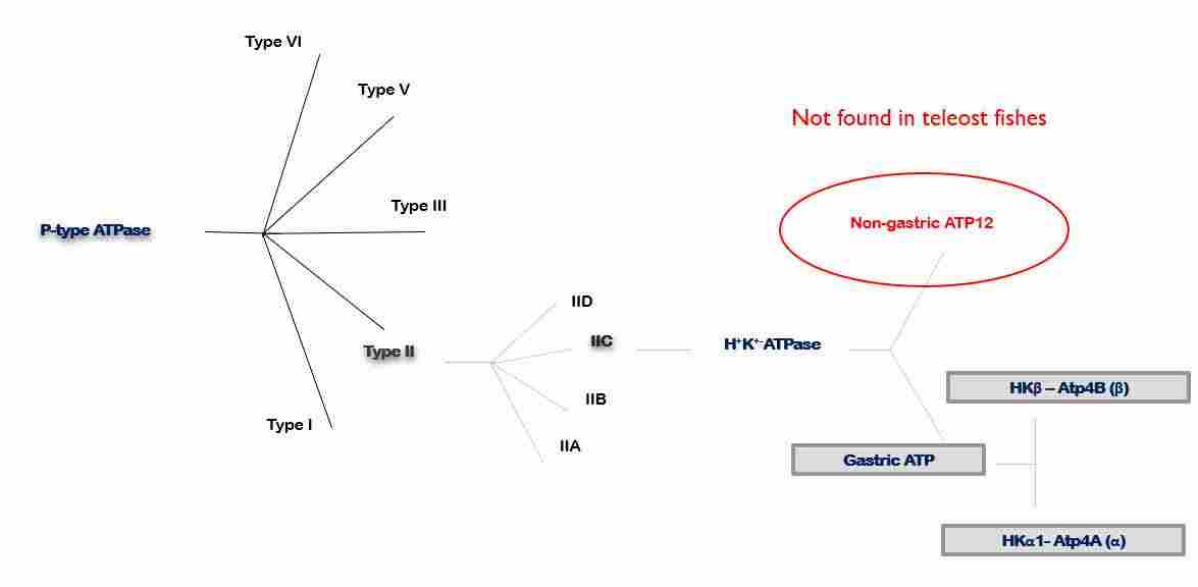

Figure 1.2. Diagram of the p-type ATPase family and subfamily showing the classification of the gHKA that found in *Oreochromis niloticus.* Shaded squares represent gastric ATP and the α and β subunits that catalyzes the hydrolysis of ATP, which is joined with the exchange of H^+ and K^+ ions across the plasma membrane that allows the transport of ions.

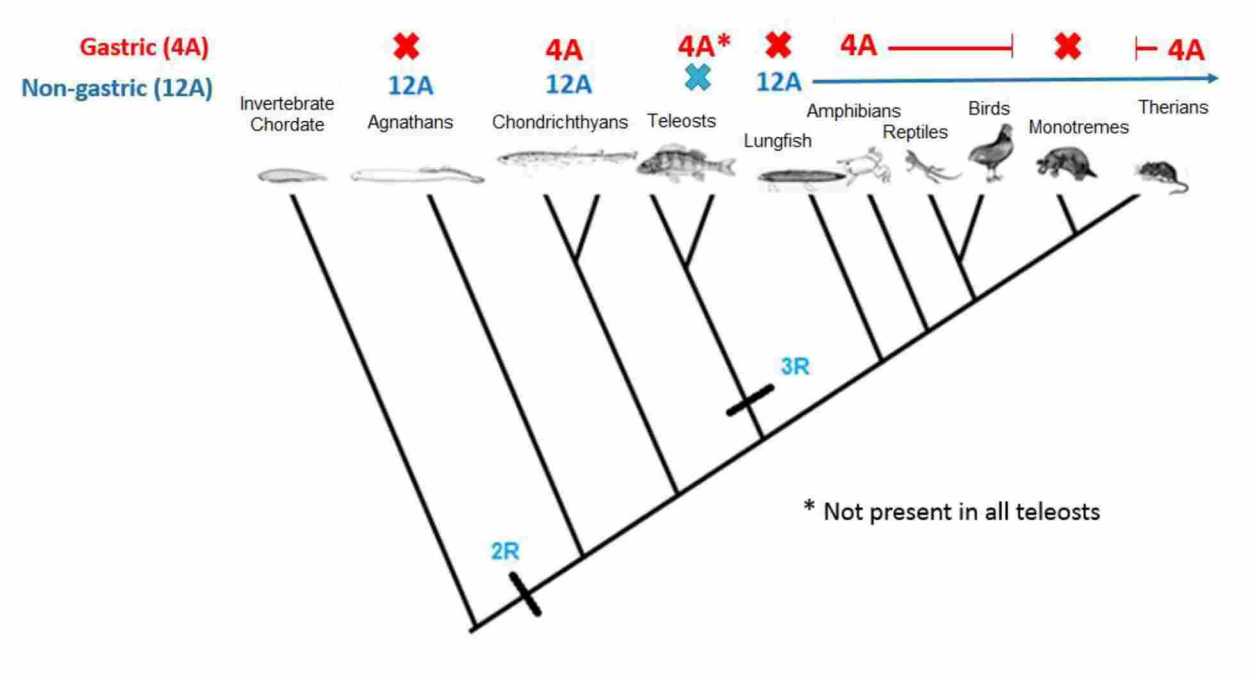

Figure 1.3. The vertebrate lineage showing the genes associated with H^+/K^+-ATPase (HKA). The *atp12a* (12A) gene corresponds to the non-gastric HKA α subunit and the *atp4a* gene corresponds to the gastric HKAα1 subunit. The 2R and 3R represent rounds of whole genome duplication found in the vertebrate and teleost ancestors, respectively. "X" represents genomic loss or absence of the *atp4a* or *atp12a* gene.

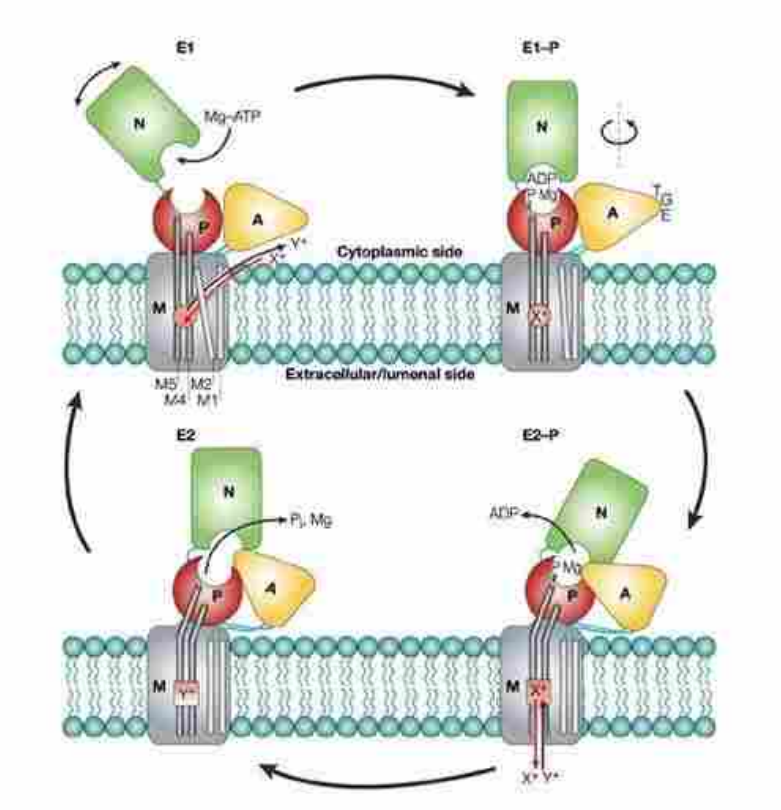

Figure 1.4. General catalytic mechanism of a P-type ATPase (Kuhibrandt 2004). The H^+/ K^+-ATPase uses the energy of ATP hydrolysis to actively pump intracellular hydrogen (H^+) out of the cell in exchange for extracellular potassium (K^+) ions against their concentration gradients. The stoichiometry of the pump changes from $2H^+$:$2K^+$:1ATP to $1H^+$:$1K^+$:1ATP at low pH. As the gastric acid pump its main role is acidifying the stomach contents.

CHAPTER 2

MATERIALS AND METHODS

2.1 Animals

Nile tilapia (*Oreochromis niloticus)* were supplied by Sand Plains Aquaculture facility (London Ontario), with average mass of 5 - 25 g for *in vivo* or 50 to 200 g for *ex vivo* experiments and were fed twice daily 2 g of Ewos pellets *ad libitum* approximately. Upon arrival, the fish were placed in 180 L tanks supplies with dechlorinated city water and reverse osmosis (RO) water at a room temperature of 25°C ± 1°C. All experiments were approved by Wilfrid Laurier University's Animal Care Committee (R14002) and followed the guidelines from the Canadian Council of Animal Care.

2.2 *In vivo* experiments

2.2.1 Rb^+ kinetics

Rubdium uptake rates were determined by measuring rubidium accumulation in muscle over time. *O. niloticus* (n=16, 6-15 g) were captured randomly from the 180 L holding tanks using a hand net, then moved to one of four tanks of 3 L (n=4 / tank) on flow through with aeration. The water pH was maintained between 7.0 and 7.8. Fish were acclimated overnight and fluxes were started by stopping the flow to the tanks and specific concentration of Rb^+ (as RbCl) were added to each tank. Then an initial water sample of 10 ml was taken and *O. niloticus* were euthanized for further samples collection over the next 12 h at intervals 0, 3, 6, and 12 h, without disturbing the fish to any major extent. Concentrations tested for Rb^+ were 0.1, 0.5, 1, and a higher concentration of 2.5 mM. At the end of the flux period *O. niloticus* were euthanized by an initial immersion in 0.2 g/L MS222. The tail was cut to collect blood in heparinized capillary tubes, and muscle samples (usually 0.2 -1g) were removed from the area below the dorsal fin. Muscle samples were weighed

and dried for 3 days at 60°C. Collected samples (plasma and dry muscle) were digested in concentrated nitric acid with a volume of a 2.5ml for muscle and 0.4ml for plasma samples. Rb^+ uptake was determined using PinAAcle 900T Atomic Absorption Spectrophotometer (Perkin Elmer Waltham MA) in flame mode. HNO3 and $CsCl_2$ were added to the samples at final concentrations of 0.1% and 0.2%, respectively. Standards ranged from 0-9.6 μM. Samples and standards were diluted 50x with milliQ (ultrapure) water and the uptake rates were calculated in μmol/g wet mass fish.

2.2.2 *In vivo* pharmacological inhibition of the proton pump with Omeprazole:

Omeprazole was used as a proton pump inhibitor to evaluate the activation of HKA for this experiment using two pairs of control and omeprazole injected fish at a time. *O. niloticus* (n=4) were moved to individual tanks of 500 mL with aerator pumps and flow through that stopped after the omeprazole was injected into the fish. Rb^+ added to each tank with a specific concentration per experiment. tested concentrations for Rb^+ were 0.1, 0.5, 1, and a higher concentration of 2.5 mM. Treatment for the omeprazole injected fish (n=6) included a 5mg/kg omeprazole dissolved in DMSO and 0.9% sodium chloride. The control (n=6) was an equivalent injection volume of 0.9% NaCl with 2% DMSO. Fish were anesthetized with 0.2 g/L of MS222, weighted and injection volume calculated. All fish were injected twice with omeprazole or vehicle, the first time was 12 h before the start of the experiment and 3or 6 hours before the terminal sampling. Fish were killed with an overdose of MS222, length and weight measured and plasma and muscle samples were collected.

2.2.3 Analytical techniques:

2.2.3.1 Ammonia and titratable acidity:

Ammonia in water samples was measured spectrophotometrically (Spectramax 190, Molecular Devices, Sunnyvale, CA) using a standard ammonia assay (Verdouw et al., 1978). Total ammonia efflux rates (J_{amm}) and Titratable acidity (J_{TA}) were measured to determine the net acid flux (J_{H+}). through the course of the experiments water was aerated for ammonia and titratable acidity measurements. A 15 mL water sample was collected at intervals (0, 3, 6, and 12 h). Using a standard ammonia assay (Verdouw et al., 1978) ammonia was measured by diluted the collected water sample 10 times to fall within the standard curve range of 0-150 μM and read at 650 nm using (Spectramax 190, Molecular Devices, Sunnyvale, CA). Total ammonia efflux rates (J_{amm}) were calculated in μmol/g/h. Titratable acidity (J_{TA}) was determined using Radiometer Copenhagen TTT80 Titrator and ABU80 Autoburret with a PHM84 pH and Hamilton pH electrode. Samples (10mL) were aerated for 1 hour prior to measurements in order to remove CO_2 and with continued aeration, titrated with 0.01 N HCl until a pH of approximately 4.5 and then brought to a final pH of 4 using 0.005 N HCl. Titrant volumes were then multiplied by the respective HCl concentration to give μmol H^+ in 10 mL water samples. The net acid flux (J_{H+}) was calculated in μmol/g/h using the relationship: $J_{H+} = J_{TA} + J_{amm}$ (Wood and Caldwell, 1978).

2.2.3.2 Rb^+ kinetics:

Rubidium uptake was determined by measuring muscle rubidium accumulation over time. Weighed and dried muscle samples were dissolved in a 2.5 ml concentrated HNO_3 and diluted 50x with MilliQ and CsCl was added to the samples at final concentrations of 0.2%. Rb^+ concentrations

of (0.1, 0.5 and 1mM) were determined using a PinAAcle 900T Atomic Absorption Spectrophotometer (Perkin Elmer Waltham MA) in flame mode. Standards were diluted 50x with 0.2%CsCl in milliQ water in a range from 0-9.6 µM.

Using the data of Rb^+ uptake rates with water conentrations of 0.1, 0.5 and 1mM that were tested, kinetics of Rb^+ were characterized using Michaelis-Menten kinetics using GraphPad Prism (version 6.01 for Windows, GraphPad Software, La Jolla, CA). Vmax (maximum velocity) and Km (concentration of the substrate when the reaction velocity is equal to one half of the maximal velocity for the reaction) were calculated by linear regression analysis of the Lineweaver - Burk plot equation when dividing 1 by each substrate (Rb concentrations) and velocity (uptakes rates). The calculated value then plotted as x-axis for 1/Substrate and y-axis for 1/velocity. The x-intercept represents -1/ Km and the y-intercept displays 1/ Vmax.

2.2.4 Statistical analyis:

Data were analyzed as mean values ± standard error the mean (s.e.m). Two-way ANOVA and t-tests were used to test for comparison and differences between treatment groups and uptake/ inhibition rates. If a significant difference was found by ANOVA, a post hoc Holm-Sidak test was done. In the case of non-normality and/or unequal variance, an equivalent, non-parametric test was used (Mann-Whitney rank sum test). Significance was accepted when $P<0.05$. All statistical analyses were carried out using SigmaPlot (11, Systat, San Jose USA).

2.3 Ex Vivo experiments:

2.3.1. Measurement of Omeprazole and SCH28080 sensitive Rb^+ uptake:

2.3.1.1 Tissue Preparation

O. niloticus (n=3) were captured randomly from the 180L tanks using a hand net, and euthanized for samples collection. The gill arches and kidney were excised and rinsed for 30 mins in pre equilibrated (99% O_2/1% CO_2) Rubidium ringer's solution (in mmol l^{-1}:140 NaCl, 15 $NaHCO_3$, 1.5 $CaCl_2$, 1.0 NaH_2PO_4, 0.8 $MgSO_4$, 5.0 D-glucose and 5.0 N-2 hydroxyethyl-piperazine propanesulphonic acid, Hepps; 310 mosmol kg^{-1}, pH 7.8). Each gill arch was then cut transversely into blocks of 3–5 pairs of filaments (5–10 mg), kidney tissue was cut into block of (4–8 mg). Pieces were placed in a Petri dish and incubated in Rb^+ Ringer for 30 mins in various RbCl concentrations of 0.1, 0.5, 1, and a higher concentration of 2.5 mM, (concentration per experiment). Following incubation, tissues were washed free of Rb^+, using Tris-sucrose buffer (in mmol l^{-1}: 2.5 KCl, 1.5 $CaCl_2$, 1.0 KH_2PO_4, 0.8 $MgSO_4$, 10 Tris, 260 sucrose, pH 7.8), equilibrated with 99% O_2/1% CO_2, for at least 30 min before the experiment. The samples were then blotted gently on filter paper, weighed to the nearest 0.1 mg and placed in 1.5ml tube. Ion extraction for samples was performed overnight for 0.5ml in 5% trichloroacetic acid (TCA) 24°C. Next day, samples were homogenized with 2 bullet blinder beads per tube using (Precellys 24 bead homogenizer). The samples were then centrifuged (14 000 xg for 15 mins at 4°C) (Thermo Scientific Sorvall Legend Micro 21R Microcentrifuge). Finally, samples were diluted 50x with milliQ and $CsCl_2$ were added at final concentrations 0.2%. Standards ranged from 1.2 to 12.25 µM. TCA and CsCl were added at final concentrations of 0.1% and 0.2% respectively. Rb^+ uptake was measured by PinAAcle 900T Atomic Absorption Spectrophotometer (Perkin Elmer Waltham

MA) in flame mode at 780.8 nm with a slit width of 2.0 nm. The rate of Rb^+ uptake was expressed as µmol/g wet mass.

2.3.1.2 Omeprazole

Samples were transferred to 24 well microplate, and supplied with Rb^+ Ringer solution contains Rb^+ concentration as RbCl that pre-gassed with 99 % O_2/1% CO_2 for 30 mins and omeprazole was added to the solution for a final concentration of 0.5 mM. The omeprazole stock solution was made at 19.2 mM in methanol. To determine an optimal inhibition time, the initial time course experiment over 0, 10, 20, and 30 min showed a linear uptake of Rb over time in the presence or absence of omeprazole. This was followed by omeprazole uptake inhibition experiments with different concentrations of Rb (0.5, 1, 1.5, 3.5 mM). The control was an equivalent volume of methanol.

2.3.1.3 SCH28080:

Gill tissue moved to a microplate 24 well, and supplied with Rb^+ Ringer solution contains Rb^+ concentration as RbCl that pre gassed with 99 % O_2/1% CO_2 for 30 min. SCH28080 (Santa Cruz Biotech) added for a final concentration of 0.2 mM. SCH28080 made at 36.06 mM and dissolved in DMSO. An initial experiment were done for the time course of Rb^+ uptake at time 0, 10, 20, 30 minute, once the acclimation stops and significant inhibition in the uptake by SCH28080 shown. Another experiment was done to evaluate flux and inhibition rate with different concentrations of RbCl 0.5, 1, 1.5, 3.5 mM. The control was an equivalent volume of DMSO.

2.3.2 Tissue viability assay (Lactate Dehydrogenase activity)

The lactate dehydrogenase (LDH) is the most commonly used enzyme to validate cell membrane integrity. The measure of the enzyme leakage can give an estimation of cell damage (death) for a sample as when the cell membrane are damaged cytosolic enzymes pass into the extracellular medium. LDH assays was performed to evaluate LDH activity in the tissue and the leakage of enzyme into the media that can be used as a marker of dead or damaged cells from treatment.

Extracellular LDH: 1ml of culture medium (Rubidium Ringer's solution) were moved from 24 microplate wells into1.5ml tube and snap frozen on dry ice.

Total LDH: Total LDH is calculated as the sum of extracellular LDH plus the intracellular (tissue) LDH. To measure intracellular LDH, tissues were placed in 24 microplate and rinsed with warm PBS (in mmol l^{-1}: 137 NaCl, 2.7 KCl, 8.5 Na_2HPO_4, 1.5 KH_2PO_4, pH 7.4) then moved to a tube and homogenized in 500ul PBS to release all intracellular LDH and then centrifuged. The LDH in the supernatant was assayed on the same day or frozen at -80ºC for later measurement.

LDH assay:

In a 96-well plate10µl of sample (tissue and medium) was added to each well containing 200 µl of 0.32 mM NADH dissolved in PB (50mM KH_2PO_4, pH 7.4). Plates were incubated for 2 min at 25ºC in the plate reader. The plate was then read after 10µl of 7.36 mM of pyruvate in PB was added as quickly as possible. The linear part for the calculation for the 'kinetic' function of the Molecular Device SpectroMax plate reader spectrophotometer using SOFTmax Pro 4.0. software was used at an absorbance at 340 nm for 10 min and a linear (negative) slope obtained.

Expression of LDH leakage as a percentage of LDH activity in the extracellular medium from the total activity in the sample considering dilutions (10x and 5x for gills and kidney respectively), and 2500µl as total volumes of extracellular medium and 500µl homogenization medium.

$$\text{LDH leakage} = \frac{\text{LDH activity in medium}}{(\text{LDH activity in medium} + \text{LDH activity in tissue})} \times 100$$

2.3.3 Statistical analyses:

Data were analyzed as mean values ± standard error the mean (S.E.M). Two-way ANOVA was used to test for comparison and differences between treatment groups and uptake/ inhibition rates. If a significant difference was found by ANOVA, a Newman Keuls post hoc test was done. In the case of non-normality and/or unequal variance, an equivalent, non-parametric test was used (Mann-Whitney rank sum test, Kruskal-Wallis). Significance was accepted when $P<0.05$. All statistical analyses were carried out using SigmaPlot (11, Systat, San Jose USA).

2.4 Immunohistochemistry (IHC):

2.4.1 Tissue preparation

Collected gill and kidney tissues from the *in vivo* experiments were placed in embedding cassettes in 3% paraformaldehyde, phosphate buffered saline (pH 7.4) fixative for 24 hours. The tissues were then transferred to decalcification solution (30% formic acid 13% sodium citrate; FASC) for 48 hours, and then transferred to 70% ethanol (histological grade) for at least 24 hours. Tissues were then embedded in paraffin using a Shandon Citadel 1000 processor (Thermo Scientific, Pittsburgh PA). The paraffin blocks were sectioned in 5 µm thin slices using a Leica

RM2125 RTS microtome, collected on to APS coated slides, air dried and stored for future use or prepared for IHC.

2.4.2 Custom polyclonal antibodies

Antigenic peptides specific for Atp4a and Atp4b were determined from the *O.niloticus* sequences from predicted amino acid sequences from the Nile tilapia genome at ensemble.org ENSONIG00000005974 and ENSONIG00000003180, respectively. To avoid cross reactivity with NKA α and β subunits, the predicted peptide sequences were screened against Onil Atp1a1 tr|I3K3G3|I3K3G3_ORENI Uncharacterized protein and Onil Atp1b3a ENSONIG00000010624, respectively. Peptide prediction, synthesis and conjugation to the carrier protein KLH were performed by Genetel (USA). The *O.niloticus* Atp4a carboxyl-terminal peptide DEIRKLGVRRHPGSWWDQELYY (aa999-1020) and Atp4b amino terminal peptide MATLKEKRTCGQRCEDFG (aa1-18) were selected. Two chickens per antigenic peptide were used. Genetel isolated IgY's from egg yolks as Atp4b B1349 and B1350 antibodies and Atp4a B1351 and B1352. Pre-immune isolated IgY's were also provided to serve as negative controls. Screening of staining in tilapia stomach gastric glands was used as a positive control of antibody specificity (Table. 3.3).

2.4.3 IHC protocol and antibodies used:

Tissues were dewaxed at 60°C for 20 min, passed through three xylene baths (5min) and an alcohol series 2x 100% (5min) and 70% (3min), following with or without antigen retrieval. This included 0.05% citraconic anhydride for 30 min at pH 7.4 at 100°C (Namimatsu et al. 2005) followed by 1% SDS/PBS treatment (Brown et al. 1996). The sections were then washed three times with H_2O (5min) and TPBS (5min). Sections were blocked in a humidity chamber for

(20min) with BLØK (Life Technologies) or 1% fish skin gelatin (6704 Sigma). Sections were probed with the primary antibodies Atp4a-B1350 and Atp4b-B1349 at 1:500 and 1:5000 for gills and kidney respectively and mouse monoclonal, for the Na^+/K^+-ATPase (NKA) α5 (1:100), negative controls included the pre-immune serum (1:500 or 1:5000) ,(1:5000) for gills and kidney respectively. Slides were incubated 1-2 h at 36°C. Then washed in three times with TPBS (5-10-15 min) with intermittent agitation. The secondary antibodies were goat to mouse IgG Alexa 555 (1:500) and goat to chicken IgY Alexa 488 (1:500) applied for 1-2 h at 37°C, final wash performed in three times TPBS adding 5ul DAPI to second wash buffer. Double sequential chicken labelling experiments were also done using secondary antibodies goat anti chicken IgY Alexa 488 (1:500), and goat to chicken IgY CF640 (1:500) antibodies. Coverslips were mounted with 1:1 glycerol PBS, pH 7.4 containing 0.1% NaN_3.

2.4.4 Imaging:

Sections were imaged using software platform for all Leica microscopes LASX, with a LEICA DM5500 B microscope and Hamamatsu C11440 Orca-Flash 4.0 digital camera.

CHAPTER 3

RESULTS

3.1 *In vivo* experiments:

Rubidium uptake was successfully measured over time at the water Rb^+ concentration of 2.5 mM of RbCl. Rb^+ uptake, as accumulation in white muscle (or plasma), shows a linear relationship over time at maximum 12 hours (Fig. 3.1). Using a range of Rb^+ concentrations from mM the data shows a Michaelis-Menten relationship and linear regression of Lineweaver-Burk plot where the Rb^+ Vmax was 20.4 μmol/g/h and the Km value was 0.4 mM (Fig. 3.2). Rb^+ uptake was not inhibited by omeprazole there were no significant differences found in Rb^+ uptake rates between sham injected and omeprazole injected *Oreochromis niloticus* (n=4, p=0.842) (Fig. 3.3).

Net acid excretion rates (J_{H+}) were measured in *O. niloticus* (n=4) treated with omeprazole, (Fig. 3.4). There was no significant difference in J_{H+} (n=4) (Fig. 3.4) between the controls and omeprazole treated *O. niloticus* (p= 0.297).

3.2 E*x vivo* experiment:

Since the *in vivo* methods performed to evaluate the activity of the gHKA in Rb^+ uptake was not sensitive enough, thus I tried another methodology using gill filaments *ex vivo*. While *ex vivo* experiments facilitate manipulating the tissues, it is difficult to keep them alive. Therefore, to determine how accurate my measurements were using this method, I verified the tissue viability over the course of the experiments.

3.2.1 Tissue viability

The appearance of the intracellular enzyme lactate dehydrogenase (LDH) in the culture medium was used as an indicator of tissue viability. The highest levels of LDH activity were found

in gill compared to kidney tissue (Table. 3.1). Gills and kidney showed stable viability all through the examination phases whether with control, or treated *O.niloticus* tissues, even at the longer times examined (30min). Gill preparations the highest leakage measured was only 0.12% in control and (0.11%) in omeprazole and these were in the initial 0 min group. All other groups were less than 0.01% and there was no significant relationship with time or treatment group. In kidney, leakage rates were also very low. The highest leakage for control and omeprazole were 0.06%and 0.04%, respectively. Consequently, no differences were found ($P \leq 0.693$).

3.2.2 Omeprazole

Rubidium uptake by gill was found over 30 min in media containing 1mM RbCl (Fig 3.5). Omeprazole in *ex vivo* treated gills significantly inhibited Rb^+ uptake (Fig 3.5). No significant differences in tissue Rb^+ concentrations were observed between 10 and 30min. In *ex vivo* kidney preparations a similar trend was observed with significant increases in tissue Rb^+ concentrations over 20 min in control tissue and a significant inhibition after 10min in omeprazole treated kidney tissue (Fig 3.6) (n=3) (P= <0.001).

Fluxes made over 15 min with Rb^+ concentrations of 0.5, 1, 1.5, 3.5 mM indicate a significant inhibition was found between control and omeprazole (n=3) in gills (Fig 3.7) and kidney (Fig 3.8) (P= <0.001). In gill, a significant inhibition was observed at 3.5 mM Rb^+ while in kidney a significant inhibition was observed at 1.5 and 3.5 mM Rb^+.

3.2.3 SCH28080

SCH28080 treated *O. niloticus* gill filaments shows a significant inhibition of Rb^+ uptake at 10 min (n=3, 2.88 ± 0.11 μmol/g/h) compared to the control (n=3, 5.75 ± 1.22 μmol/g/h) (P= <0.001) (Table. 3.2). Kidney was not measured.

3.3 Immunohistochemistry:

Stomach was used as a positive control tissue for staining specific for gastric glands only was observed with the Atp4a antibody B1352 and the Atp4b antibody B1349 (Fig. 3.9). The antibodies B1351 and B1350 showed additional non-specific staining in the stomach mucosal epithelium and were therefore not used for gill and kidney staining experiments.

Using standard IHC techniques, the staining with polyclonal Atp4a and/or Atp4b antibodies (1:250) on gills and kidney showed nonspecific staining all over the gills lamella, and few distal tubules of the kidney tissue were stained (data not shown). It was necessary to introduce a number of protocol modifications to improve the specificity of the staining. This included the following optimizations: 1.) increasing dilutions to 1:5000 and 1:500 for gills and kidney respectively, 2.) using Fish Skin Gelatin as a blocking medium instead for BLØK for gills tissue improved the staining while no differences were shown in kidney. 3.) Incubation times was dropped down to 1-2 hour rather than overnight, 4.) finally the staining was done without the antigen retrieval steps (0.05% citraconic anhydride (Namimatsu et al., 2005) and 1% SDS/PBS (Brown et al., 1996)), consequently, better staining quality was observed in both gills and kidney.

The gills of tilapia have a typical teleost gill structure of filaments with thin lamellae. Ionocytes, identified by NKA staining, were present mainly in the filament epithelium with a round shape. Immunolocalization of both Atp4a and Atp4b was found in the apical region of these

ionocytes (Fig 3.10 and Fig. 3.11). The appearance of staining varied from diffuse apical to restricted along the apical membrane.

The kidney of Nile tilapia has glomeruli and nephrons with a proximal, distal and collecting tubule and duct. The different regions can be distinguished based on tubule cell morphology and Na^+/K^+-ATPase immunolocalization. In proximal tubule, Na^+/K^+-ATPase is weak and restricted to the basal membrane, distal tubule has the strongest Na^+/K^+-ATPase staining in a basolateral location, while the collecting tubule/duct has weak Na^+/K^+-ATPase staining but in a basolateral location. H^+/K^+-ATPase staining with both Atp4a and Atp4b antibodies was found apically in the collecting tubule and absent from proximal and distal tubule regions (Fig 3.12.A and Fig 3.12.B).

Through the double labeling techniques, the antibodies showed clear apical overlapping in staining to the ionocytes in gills (Fig 3.13A,B) and intercalated cells in the kidney's collecting tubule segment (Fig 3.13C,D).

No difference were shown with stained omeprazole tissues in kidney (Fig 3.14 C,D), however, in gill staining in ionocytes becomes more diffuse throughout the cell although there is still apical staining observed (Fig 3.14 A,B).

By comparison, negative control pre-immune IgYs showed no staining comparable to either Atp4a or Atp4b antibodies and this was not affected by changes in the IHC conditions (Fig. 3.15) Also pre-incubation of antibodies with excess peptides eliminated specific staining (data not shown).

Table.3.1. LDH activity in gills and kidney U/g and leakage percentage into the medium in control (Ctrl) and omeprazole (OMZ) treatment groups over time (n=3) *Oreochromis niloticus* (Two way ANOVA, P =0.693)

Time	**Ctrl**		**OMZ**	
Gill	**U/mg**	**% leak**	**U/g**	**% leak**
0	82.9 ± 6.8	0.12% ± 0.05%	84.6 ± 5.0	0.11% ± 0.05%
10	61.9 ± 7.7	0.01% ± 0.01%	97.1 ± 1.1	0.04% ± 0.04%
20	76.8 ± 6.8	0.01% ± 0.01%	85.5 ± 3.8	0.00% ± 0.00%
30	88.8 ± 5.9	0.02% ± 0.01%	92.3 ± 3.2	0.01% ± 0.01%
	Ctrl		**OMZ**	
Kidney	**U/mg**	**% leak**	**U/g**	**% leak**
0	43.1 ± 11.9	0.04% ± 0.02%	60.2 ± 4.8	0.02% ± 0.02%
10	61.9 ± 8.0	0.00% ± 0.00%	45.1 ± 6.7	0.00% ± 0.00%
20	43.8 ± 6.0	0.06% ± 0.06%	42.4 ± 6.4	0.01% ± 0.01%
30	44.5 ± 12.6	0.00% ± 0.00%	48.1 ± 6.3	0.05% ± 0.05%

Table 3.2. *Ex vivo* gill Rubidium (Rb^+) inhibition rate with SCH28080 at 10 min. ± s.e.m in control and the inhibitor added (n=3) *Oreochromis niloticus* (µmol/g wet weight). * Represents statistically significant difference from Omeprazole (t-test, P = 0.001)).

Treatments	**Rb^+ (umol/g/h)**
Control	5.75 ± 1.22
SCH28080	2.88 ± 0.11*

Table 3.3. Antibodies used for immunohistochemistry staining.

Target	Antibody	Dilution	Secondary
Atp4a (HKα1)	B1351	1:100-1:5000	Goat anti-chicken CF640
Atp4a (HKα1)	B1352	1:100-1:5000	Goat anti-chicken CF640
Atp4b (HKβ4)	B1349	1:100-1:5000	Goat anti-chicken CF640
Atp4b (HKβ4)	B1350	1:100-1:5000	Goat anti-chicken CF640
Chicken pre-immune IgY	-	1:100-1:5000	Goat anti-chicken CF640
Normal rabbit serum	-	1:500	Goat anti-rabbit Alexa
Mouse negative control	J3	1:100-1:5000	Goat anti-mouse Alexa
Atp1a1 (NKα1)	α5	1:500	Goat anti-mouse Alexa
Atp1a1 (NKα1)	αR1	1:100	Goat anti-rabbit Alexa
Slc12a1/2/3 (Nkcc/Ncc)	T4	1:100	Goat anti-mouse Alexa

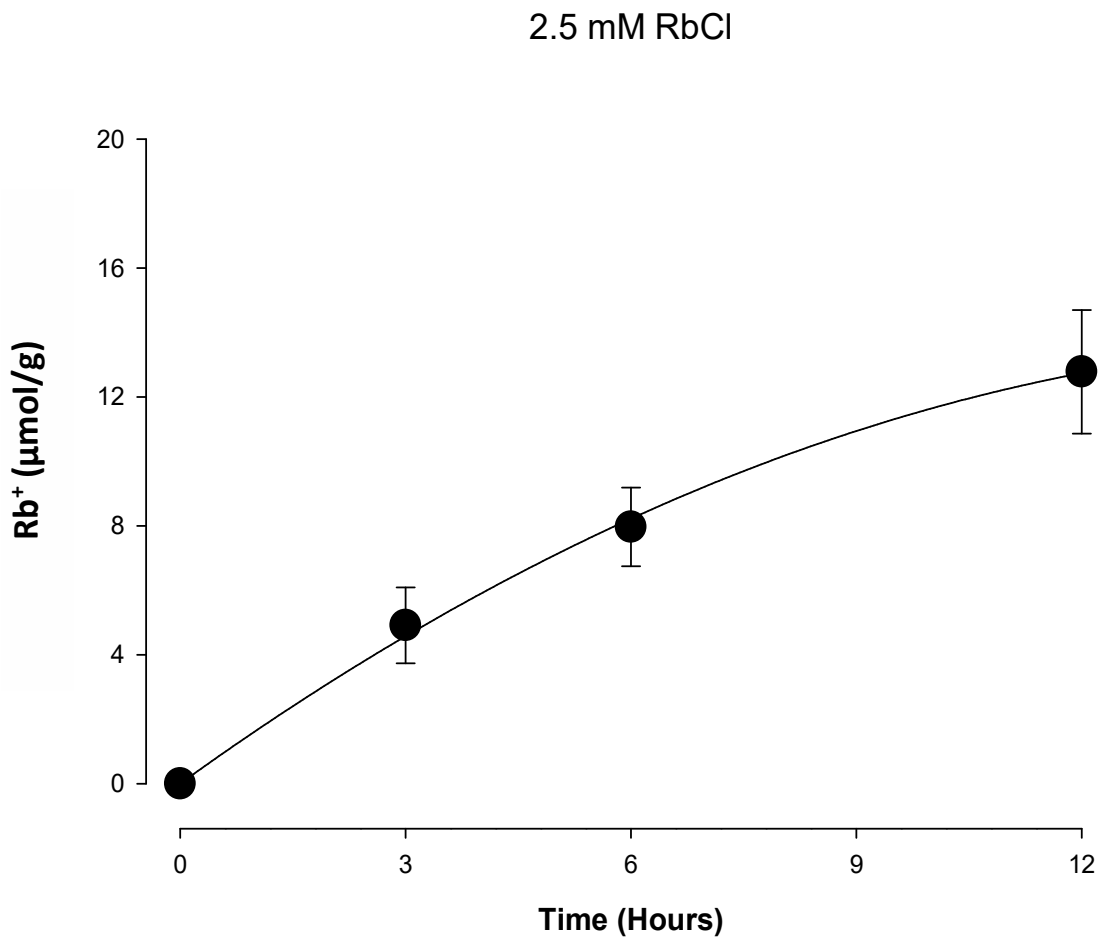

Figure 3.1. Rubidium (Rb^+) uptake in (*Oreochromis niloticus)* measured over 12 hours at 3 hours intervals during exposure to 2.5mM RbCl (n=9). One way ANOVA.

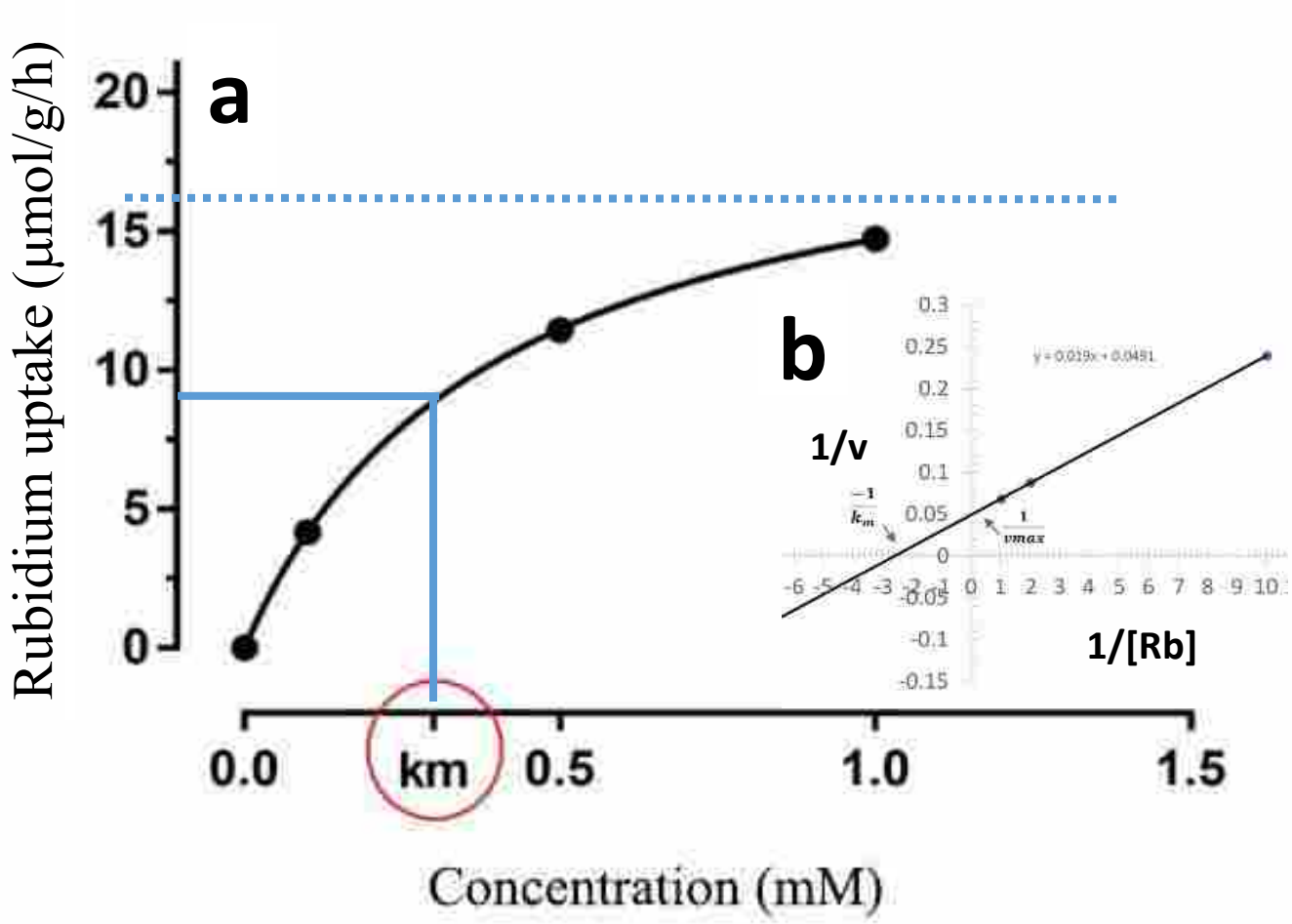

Figure 3.2. *In vivo* rubidium (Rb^+) uptake in (*Oreochromis niloticus)* for range of concentrations of rubidium chloride. Uptake kinetics of Rb^+ were characterized using Michaelis-Menten kinetics using GraphPad Prism (version 6.01 for Windows, GraphPad Software, La Jolla, CA). **(b).** Vmax=20.4 and Km=0.4 were calculated by linear regression analysis of Lineweaver-Burk plot equation.

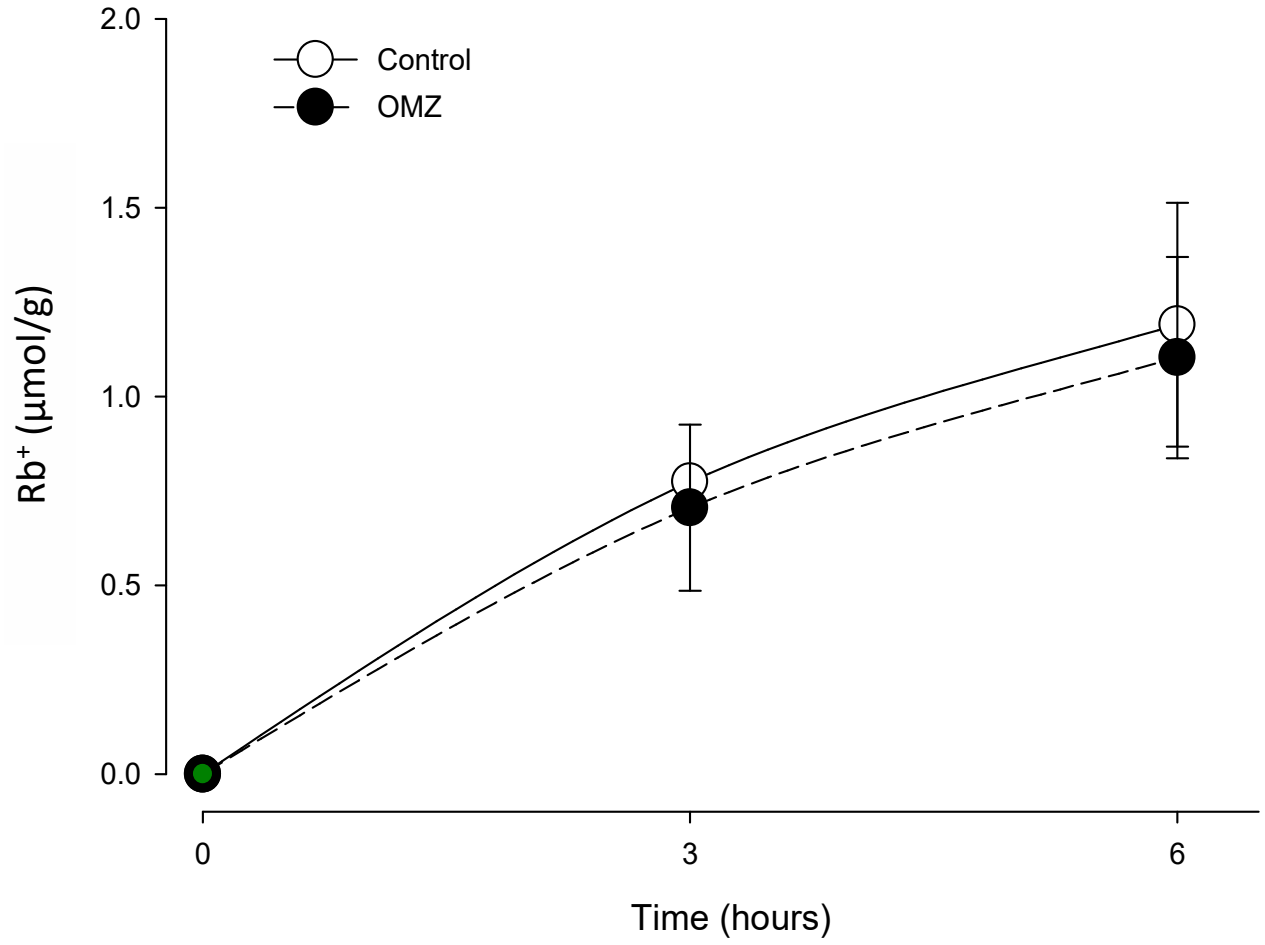

Figure 3.3. Effects of omeprazole (OMZ) injection by *Oreochromis niloticus* (solid symbols) on Rb^+ uptake over time. Control injected *O.niloticus* denoted by (open symbols). No significant differences in the uptake rate with Omeprazole were observed (P = 0.842), Two -way ANOVA.

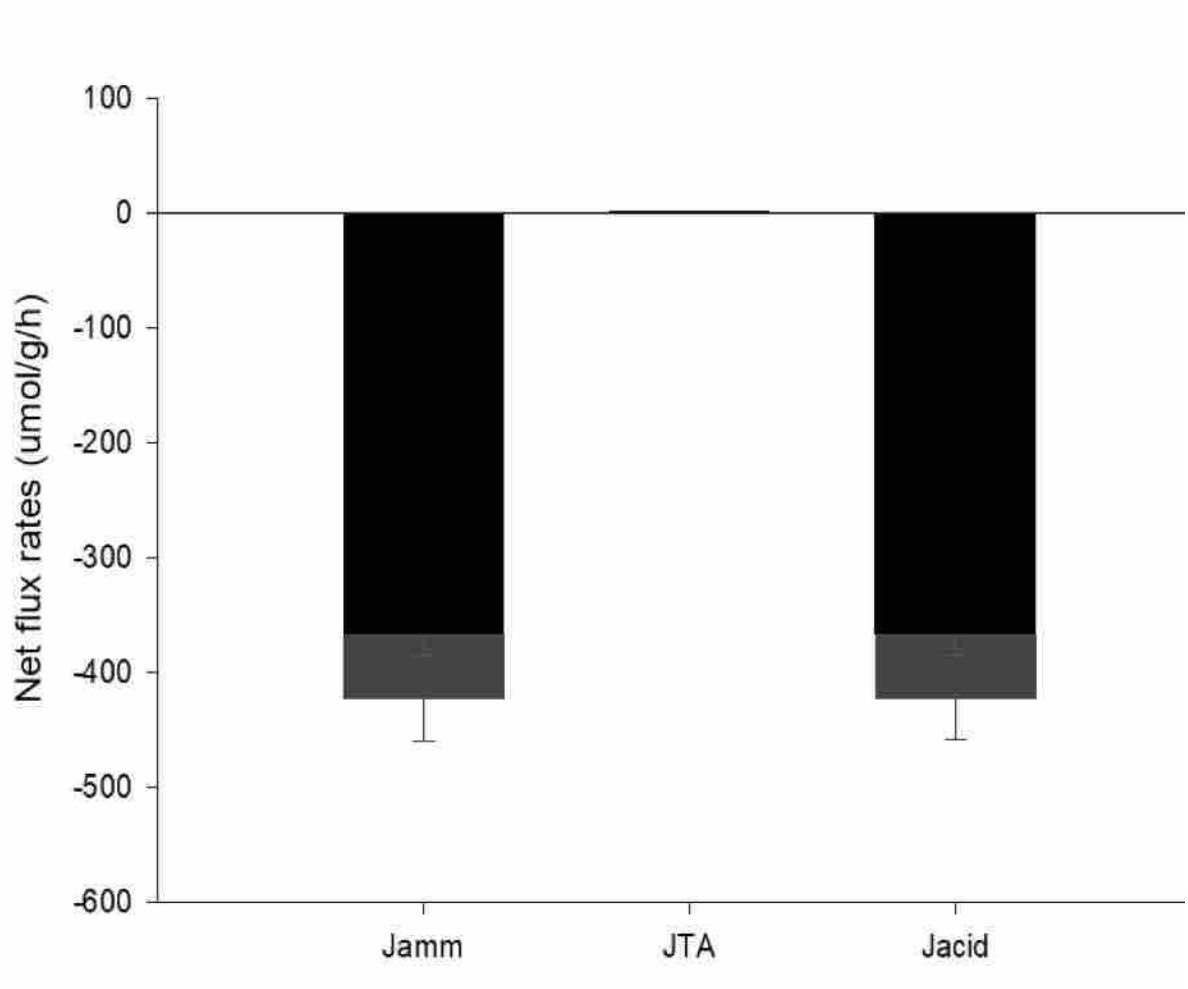

Figure 3.4. Net flux rates of ammonia, titratable acidity, and net acid (black Omeprazole; gray Control) in *Oreochromis niloticus* (n=4). Positive values indicate uptake while negative values indicate excretion. T-test.

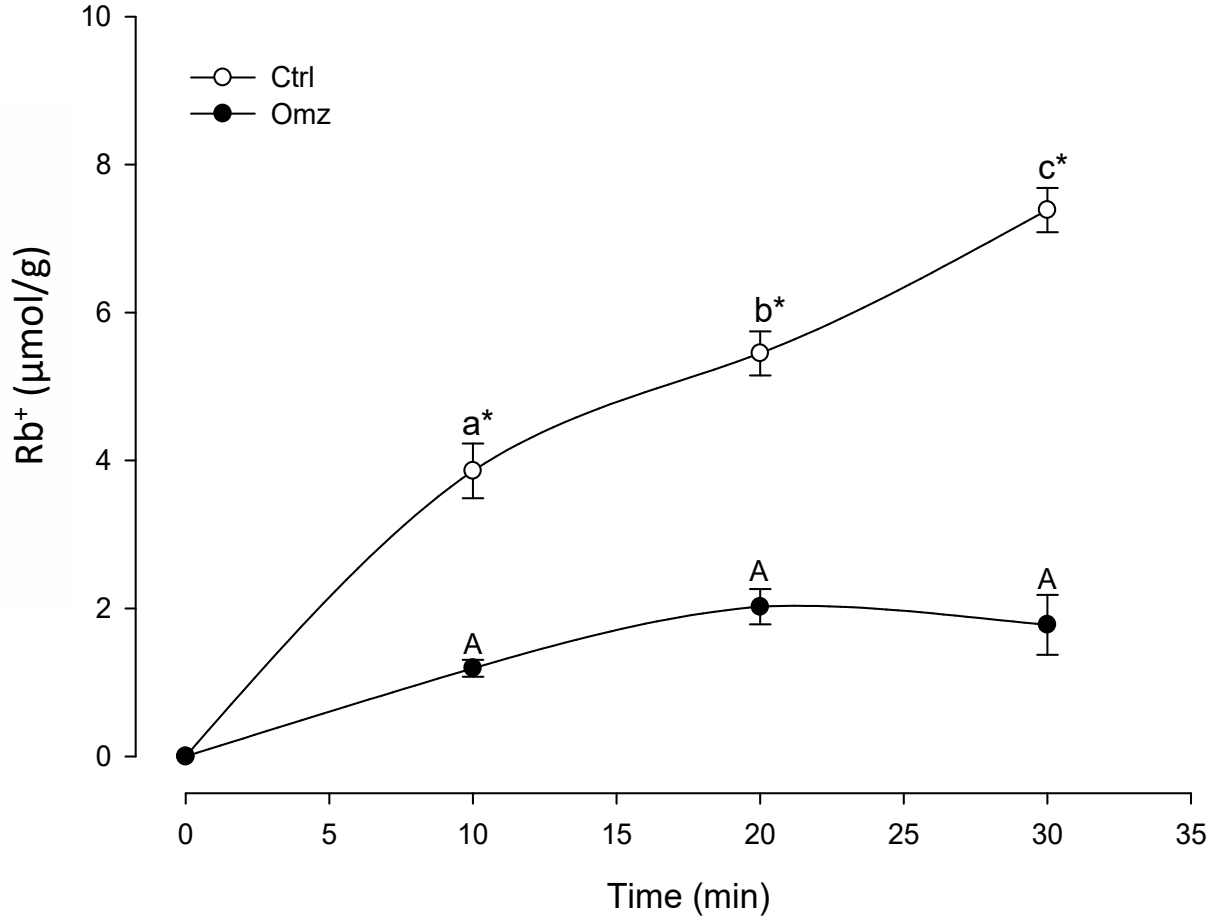

Figure 3.5. *Ex vivo* effect of omeprazole (OMZ; solid symbols) on accumulation of rubidium (Rb^+) in isolated gills filaments of *Oreochromis niloticus* over 30 min. (open symbols) represent control and different letters represent significant differences overtime within each treatment group (Control, lower case; Omeprazole upper case; P= <0.001). An asterisk (*) indicates a significant difference between Control and Omeprazole treatment group at a given time point. Two-way ANOVA, Student Newman Keuls post hoc test.

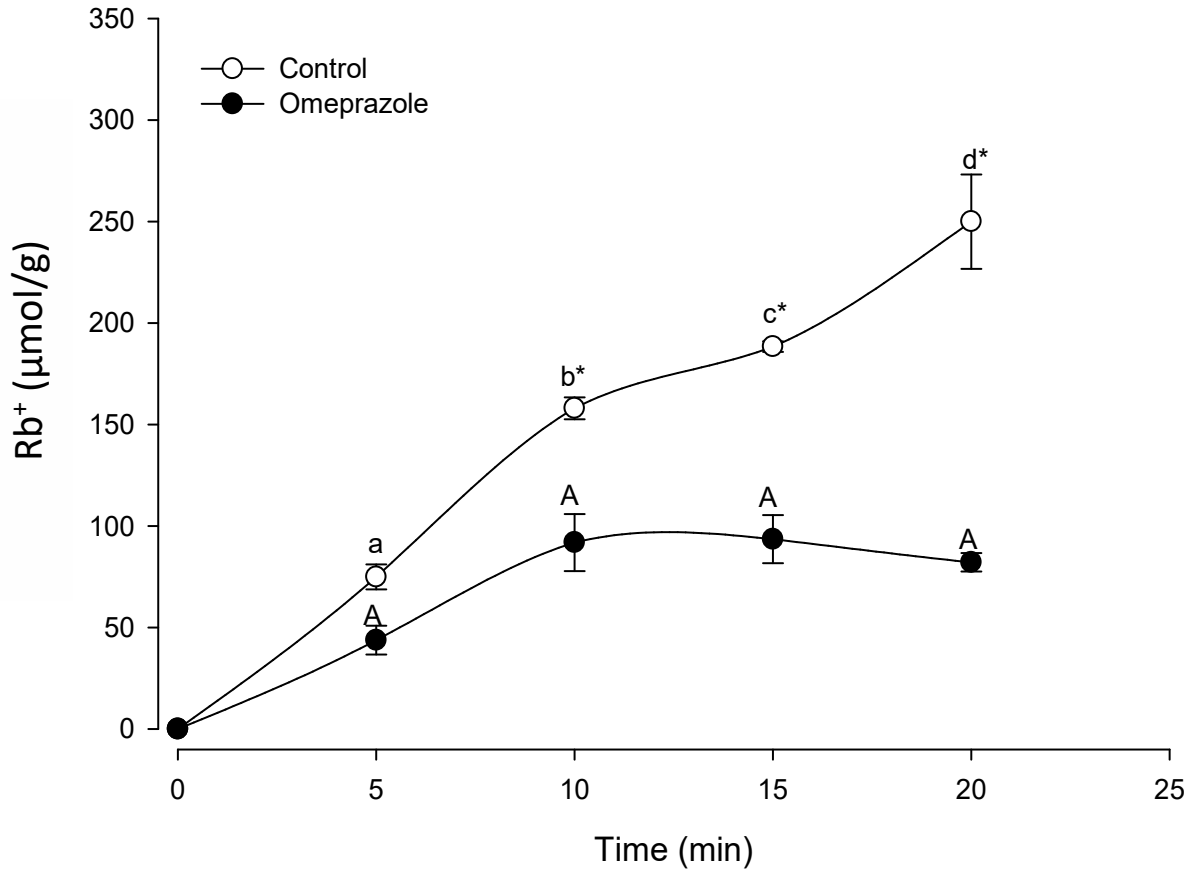

Figure 3.6. *Ex Vivo* rubidium (Rb^+) accumulation in the presence and absence of omeprazole in isolated kidney pieces of (*Oreochromis niloticus)* over 20 min. Different letters represent significant differences overtime within each treatment group (Control, lower case; Omeprazole upper case; P= <0.001). An asterisk (*) indicates a significant difference between Control and Omeprazole treatment group at a given time point. Two-way ANOVA, Student Newman Keuls post hoc test.

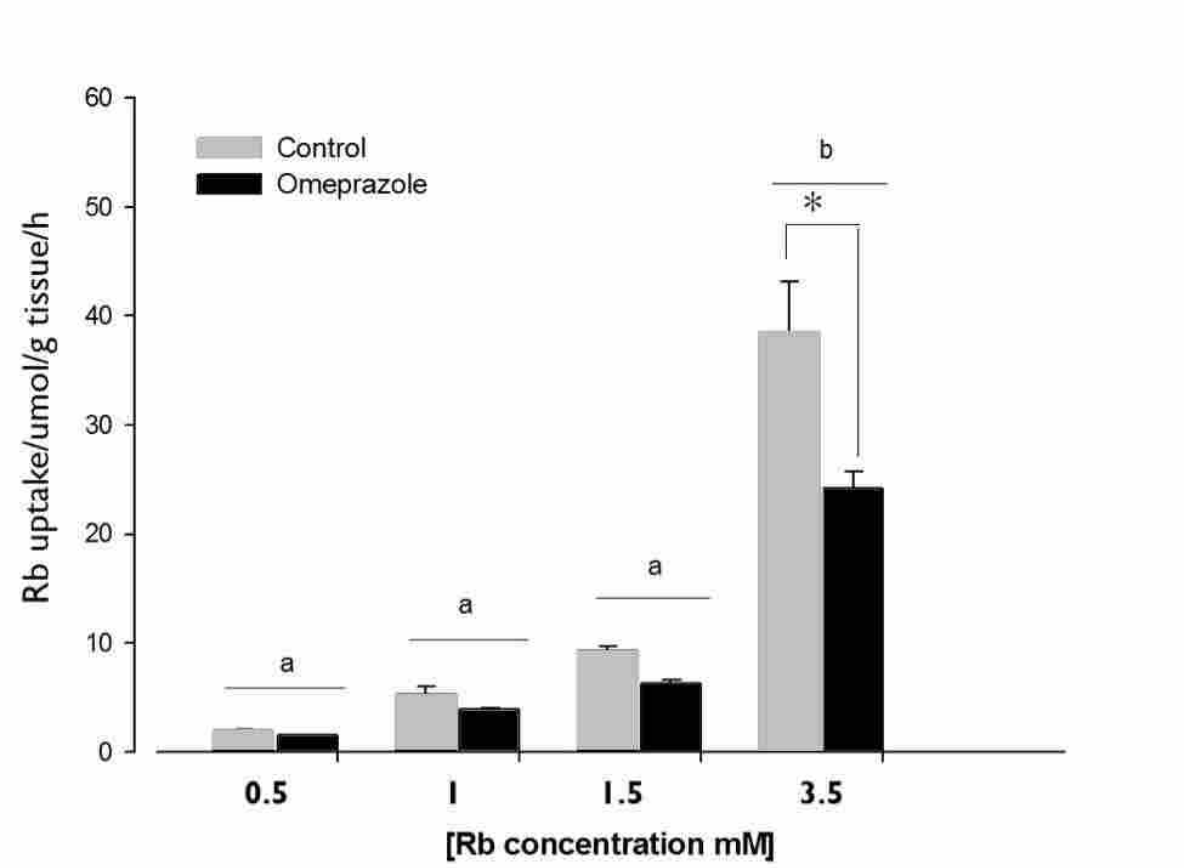

Figure 3.7. *Ex Vivo* gills rubidium (Rb^+) uptake and Omeprazole inhibition rates (*Oreochromis niloticus)* at different Rb^+ concentrations. Different letters represent significant differences between Rb^+ uptake rates at different Rb^+ concentrations. Asterisks (*) indicates a significant difference between Control and Omeprazole treatment groups at a given Rb^+ concentration [(P= <0.001). Two-way ANOVA, Student Newman Keuls post hoc test].

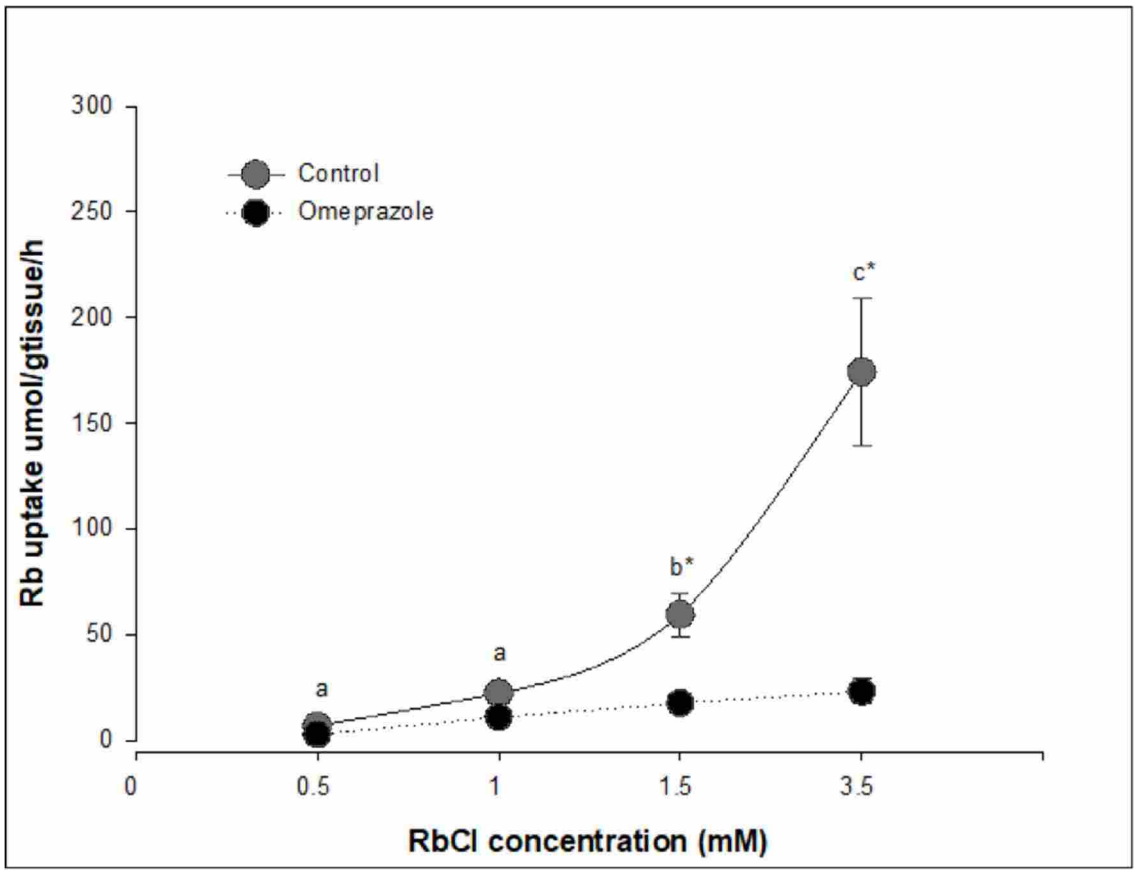

Figure 3.8. *Ex Vivo* kidney rubidium (Rb^+) uptake in the presence (open circle) and the absence (solid circle) of omeprazole of (*Oreochromis niloticus)* at different Rb^+ concentrations. Different letters represent significant differences between Rb^+ uptake rates at different Rb^+ concentrations. Asterisks (*) indicate a significant differences between Control and Omeprazole treatment group at a given Rb^+ concentration [(P= <0.001), Two-way ANOVA, Student Newman Keuls post hoc test].

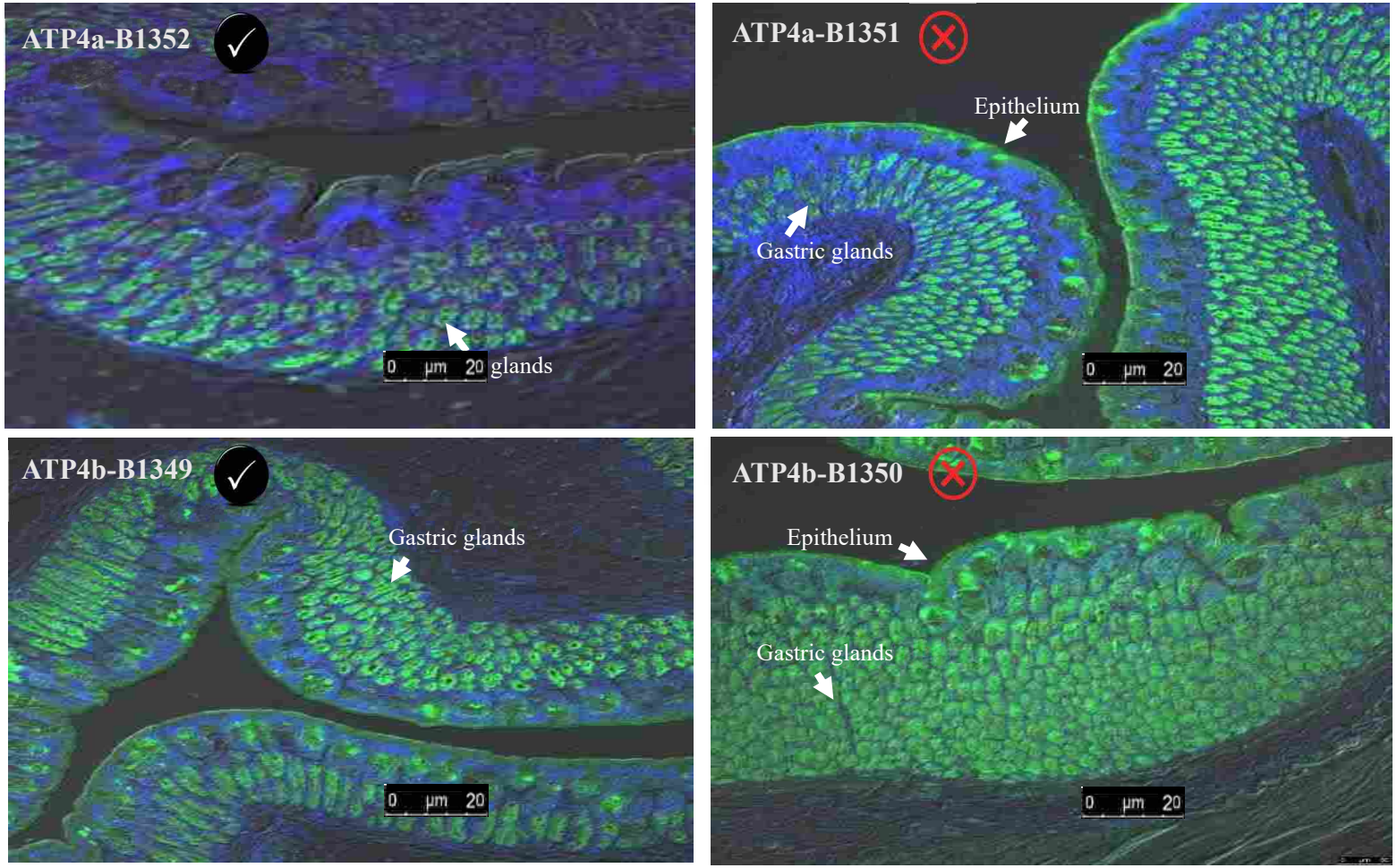

Figure 3.9. Immunohistochemistry of *O. niloticus* stomach with different antibodies for the gastric H^+/K^+-ATPase α (Atp4a: B1351 and B1352) and β (Atp4b: B1349 and B1350) subunits showing a better specific staining for the gastric glands with Atp4a-B1352 and Atp4b-1349. Scale bar 20 µm.

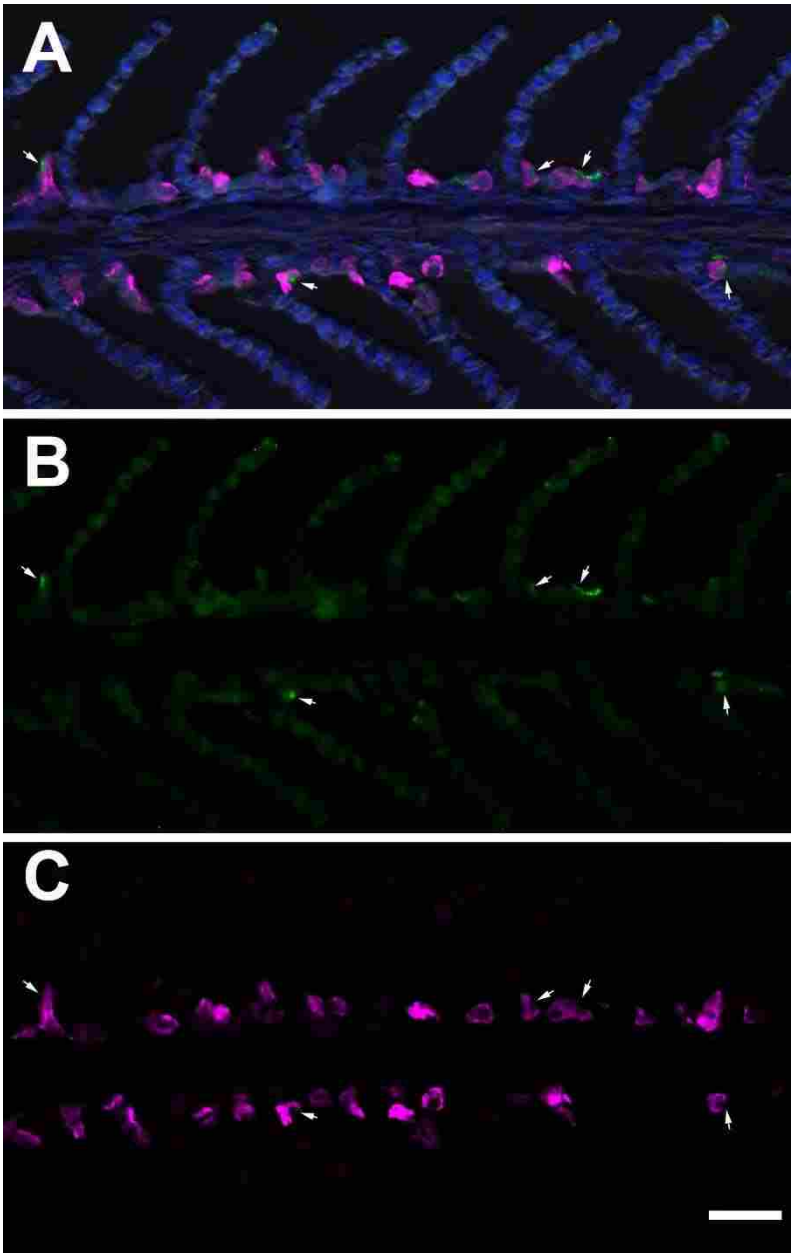

Figure 3.10. Immunohistochemistry staining of *O. niloticus* gill with (**A,B**) Atp4b-B1349 (Green) and (**A,C**) Na^+/K^+-ATPase (Fuchsia) with DAPI (Blue) and DIC overlay (**A**). Arrows indicate Atp4a positive NKA immunoreactive ionocytes. Scale bar 25 μm.

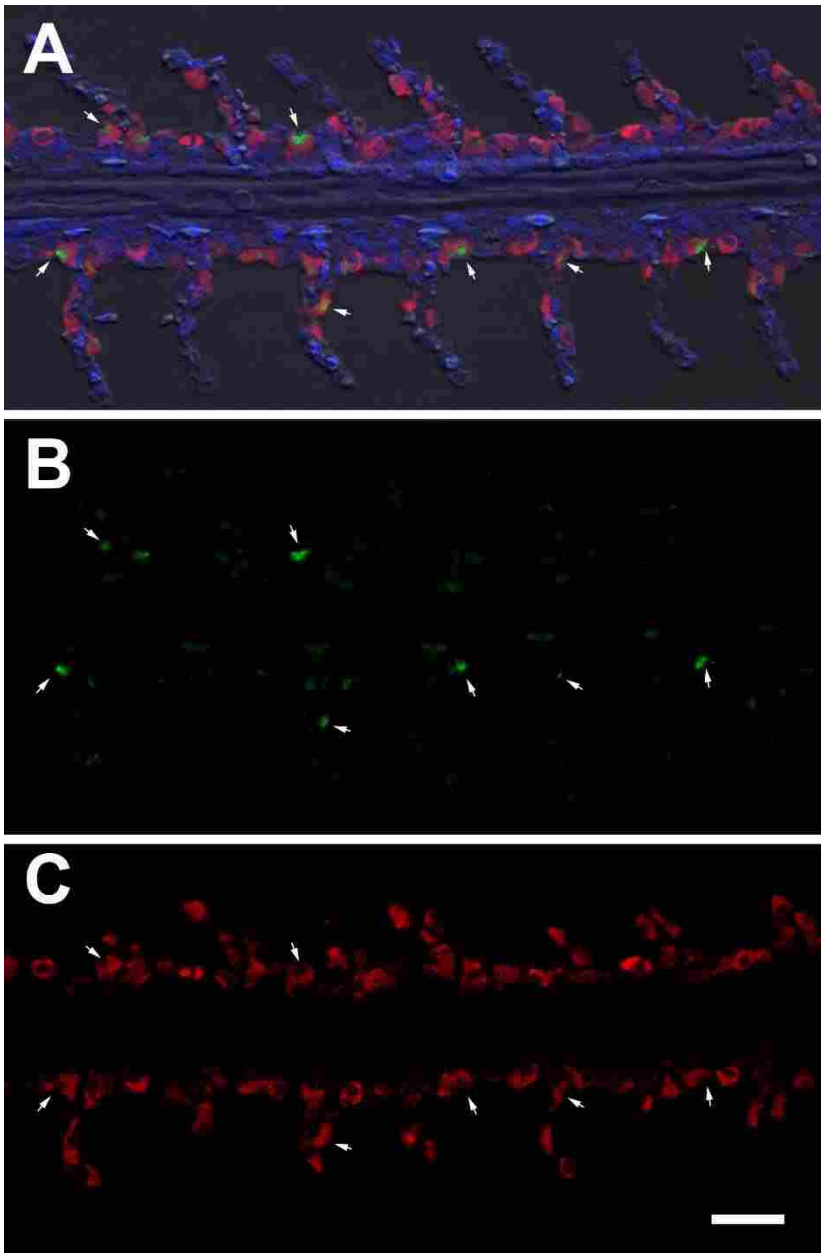

Figure 3.11. *Immunohistochemistry staining* of *O. niloticus* gill with (**A,B**) *Atp4a-B1352* (Green) and (**A,C**) Na^+/K^+-ATPase (Red) with DAPI and DIC overlay (**A**). Arrows indicate Atp4a positive NKA immunoreactive ionocytes. Scale bar 25 µm.

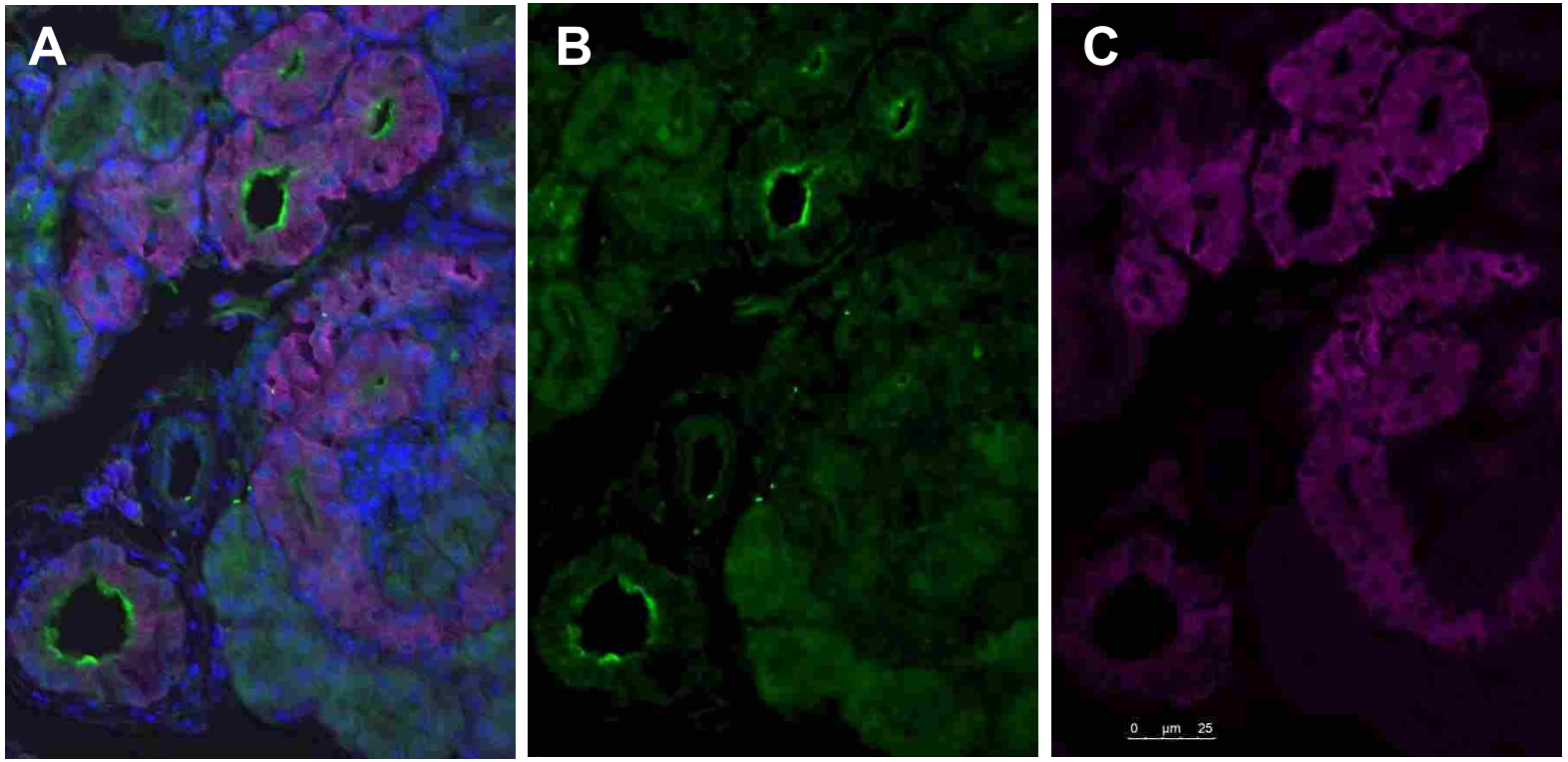

Figure 3.12.A. *Immunohistochemistry staining* of *O. niloticus* kidney with (**A,B**) *Atp4a-B1352* (Green) and (**A,C**) Na^+/K^+-ATPase (Fuchsia) with DAPI and DIC overlay (**A**). Scale bar 25µm.

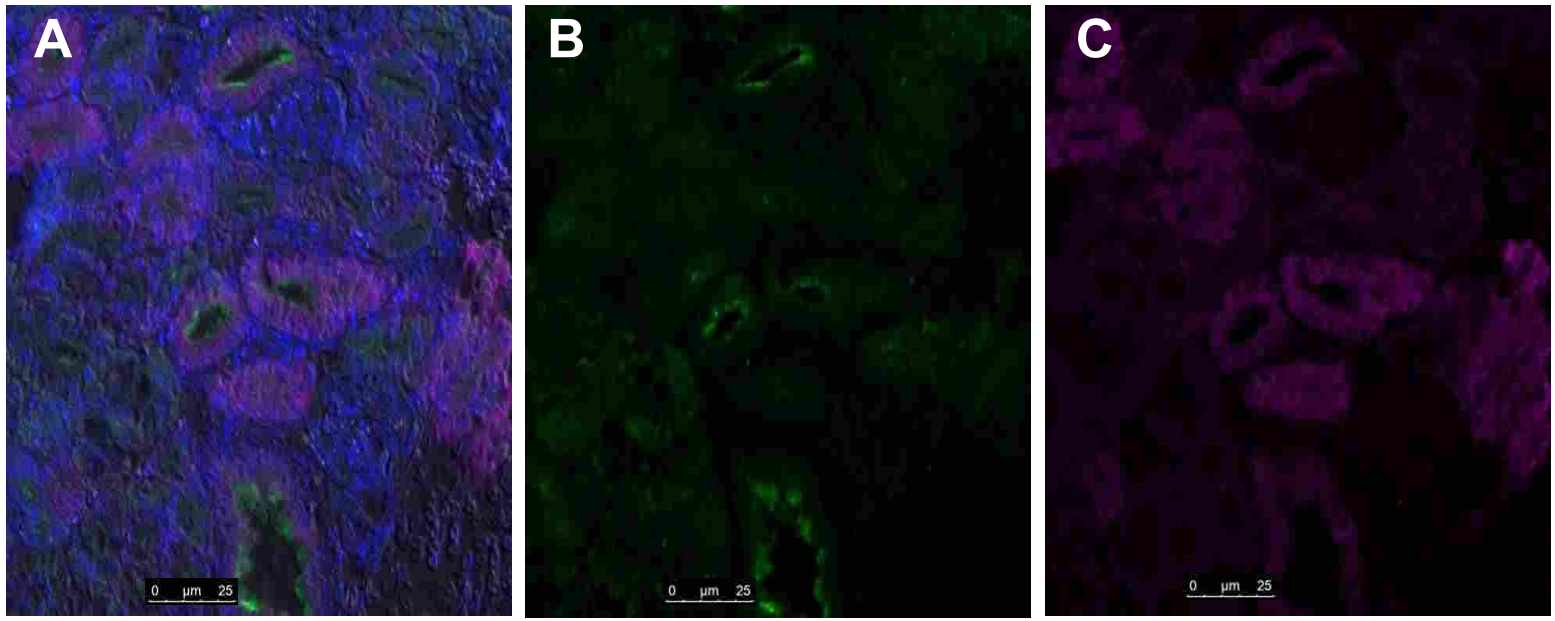

Figure 3.12.B. *Immunohistochemistry staining* of *O. niloticus* kidney with (**A,B**) Atp4b-B1349 (Green) and (**A,C**) Na^+/K^+-ATPase (Fuchsia) with DAPI and DIC overlay (**A**). Scale bar 25 µm.

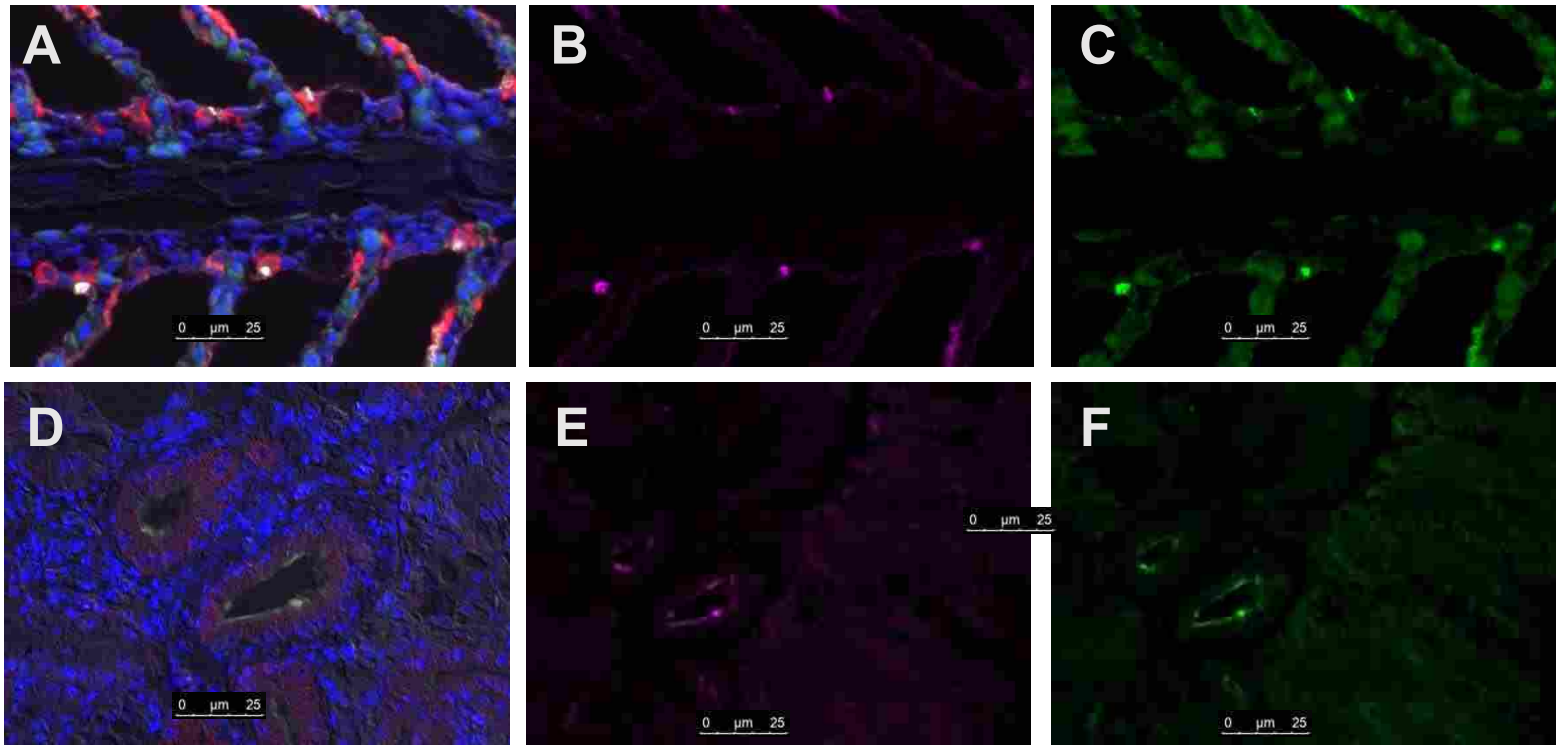

Figure 3.13. *Immunohistochemistry* ***double labeling*** *staining* of *O. niloticus* gill and kidney with (**A,C**) *Atp4a-B1352* (Green), (**A,B**) Atp4b-B1349 (fuchsia), with DAPI and DIC overlay (**A**), Scale bar 25µm.

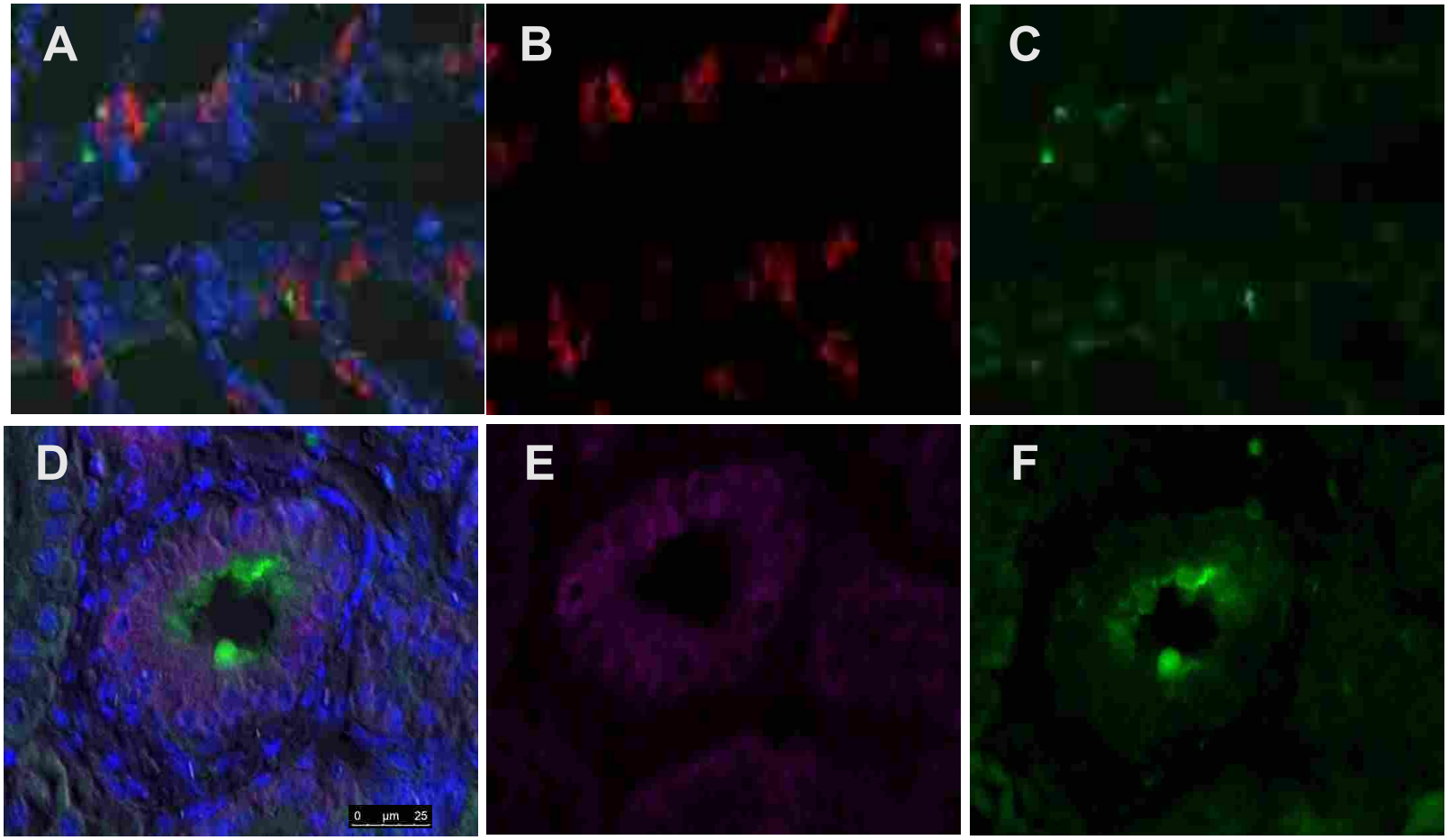

Figure 3.14. *Immunohistochemistry staining* of omeprazole injected *O. niloticus* gill (**A-C**) and kidney (**D-F**) with (**A,C,D,F**) *Atp4a-B1352* (Green), (**A,B,D,E**) Na^+/K^+-ATPase (fuchsia), with DAPI and DIC overlay (**A,D**), Scale bar 25µm.

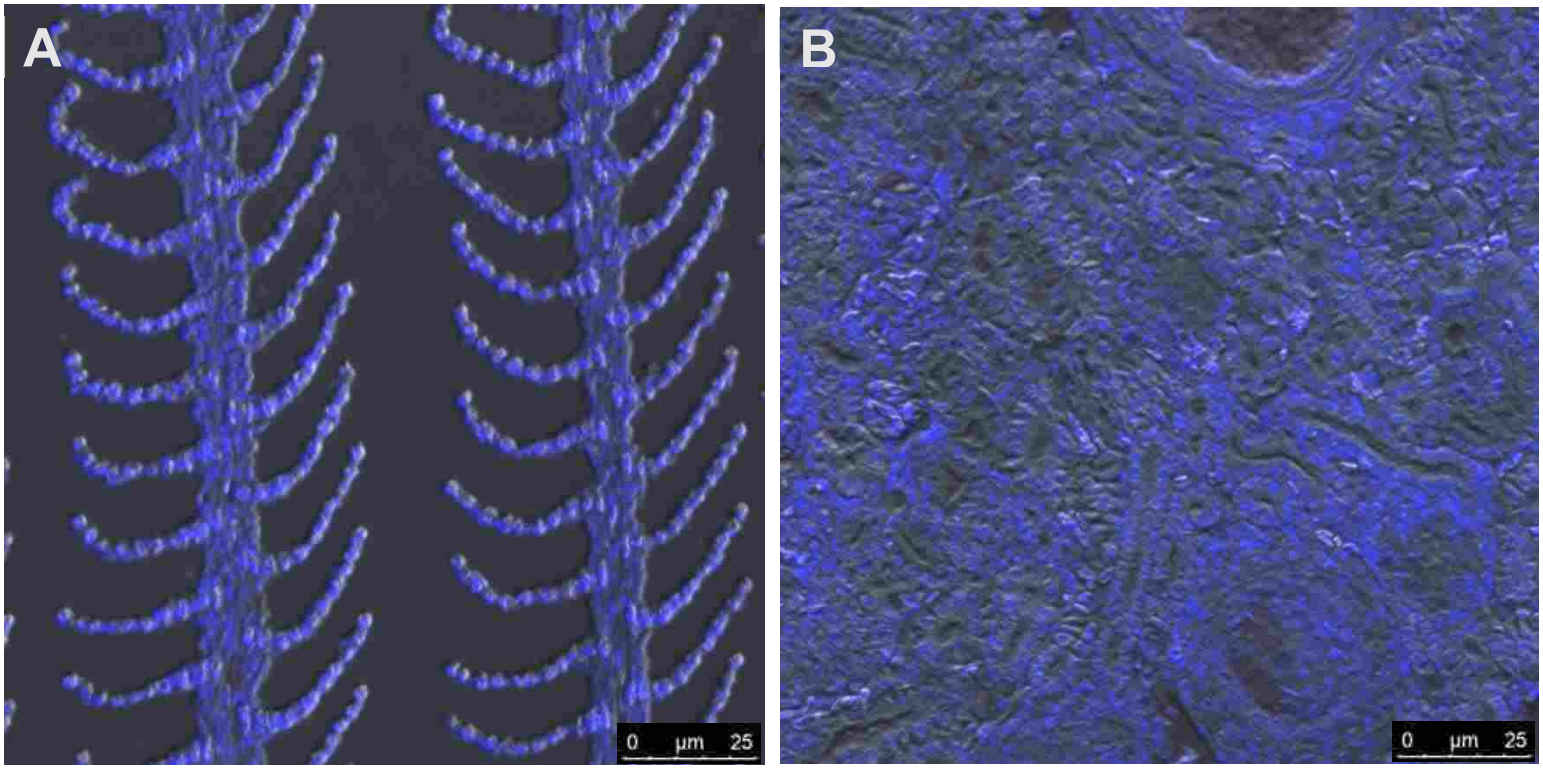

Figure 3.15. *Immunohistochemistry* staining of *O. niloticus* **(A)** gill, and **(B)** kidney with negative control pre-immune serum, Scale bar 25µm.

CHAPTER 4

DISCUSSION

In my thesis I show here for the first time, the expression and possible role of the H^+/K^+-ATPase in gill and kidney of a teleost *O.niloticus* functioning as an extra gastric HKA proton pump based on *in vivo* and *ex vivo* experimental approaches and immunohistochemistry. The *in vivo* and *ex vivo* experiments used rubidium as a surrogate flux marker for potassium uptake and carrier-mediated uptake was demonstrated *in vivo* and pharmacological inhibition by omeprazole and SCH28080 *ex vivo* in kidney and gill. It is well recognized in tetrapods that the stomach is the primary organ for acid secretion mediated by the proton pump H^+/K^+-ATPase. Consequently, in my thesis stomach was used as a positive control to validate custom made H^+/K^+-ATPase α and β subunit antibodies to confirm the molecular identity of the extra gastric proton pump in gill and kidney. Specific gastric glands immunoreactivity was observed in *O. niloticus* stomach confirming antibody specificity, whereas staining was found apically in gill ionocytes and kidney collecting duct consistent with the roles of these cells in ion and acid-base regulation. The kidney immunoreactivity in the collecting duct segment was consistent with the contribution to K^+ regulation through reabsorbing K^+ and acidifying the tubular fluid seen in mammals (Koeppen, 2009; Wingo & Cain, 1993). Taken together my results strongly support the presence (IHC) and function (Rb uptake) of the HKA in gill and kidney potassium regulation.

4.1 *In vivo*

This thesis demonstrated that the uptake of potassium by the tilapia gill was carrier mediated. The V_{max} and the apparent K^+ affinity K_m in *O. niloticus* showed a direct, substrate independent mechanism or/and a carrier mediated potassium uptake showing an acclimation of K^+ that increased gradually over time. In rainbow trout, K^+ uptake has also been measured although the mechanism has not yet been described (Eddy 1975; Gairdaire et al. 1991,1992). Eddy (1975)

reported that in trout K^+ uptake rates were only 3-5% of Na^+ and Cl^- (Eddy, 1985); however, in studies with lungfish and lamprey Rb^+ flux rates were 20% and 10% of Na^+ and Cl^-, respectively (Doherty 2016; Wilkie et al. 1998, 2001). In tilapia Rb^+ uptake rates were approximately 11 umol/kg/h, which was approximately 3% of Na^+ uptake rates (*O. mossambicus* 360 μmol/kg/h Flik et al. 1989) and in agreement with the observation made by Eddy (1985).

Several classes of drugs have been investigated using gastric glands to evaluate the activation of the pump by inhibiting the acid secretion of H^+/K^+-ATPase such as for example Omeprazole, Ouabain, SCH2808 and Vanadate (Hersey *et al.*, 1988). However, in this thesis only omeprazole and SCH28080 were tested for pharmacological inhibition experiments since these PPIs have highest binding affinity and covalent binding with H^+/K^+-ATPase (Singh *et al.*, 2013). They are widely used for treating all acid secretion related disorders in the stomach, and omeprazole was the first clinically useful acid activated drug. However, it cannot be activated at neutral pH, and its activation is related to the pH level, in view of other factors including: dosage and duration of treatment (Shin, 2010). According to Shin et al. (2009), SCH28080 was a compound developed to control acid secretion by gastric glands; however, unlike omeprazole it does not required acid activation to effectively reduce the acid secretion of the H^+/K^+-ATPase. The role of the pumps in potassium uptake based on pharmacology was demonstrated by pharmacological inhibition experiments using a proton pumps inhibitor at a concentration predicted to be sufficient in inhibition the HKA. However, only the *ex vivo* methods showed a definitive result. Whereas the final analysis for the *in vivo* results show no clear pharmacological support for the hypothesis that the gastric H^+/K^+-ATPase play a role in acid-base or K^+ regulation by the gills of *O.niloticus*.

Omeprazole is available in both oral and injectable forms (Worden and Hanna 2017). Although less common, the injectable form is an effective means of gastric ulcer treatment and gastric acidification inhibition (Worden and Hanna 2017). In the experiment 40mg/kg omeprazole was injected intraperitoneally overnight 12 h before the experiment and then at the beginning of the experiment. However, since no inhibition of Rb uptake was observed, (i) I assumed that either the time was not sufficient for the drug to reach to gills considering the duration of acid inhibition which is 48 hours allowing for strong binding to the H^+/K^+-ATPase (Shin et al., 2009); (ii) the drug was not activated since binding and inhibition of omeprazole is dependent on acidification (iii) or maybe it was cleared and excreted by the fish.. The second option is supported by a study of Shin (2010) which indicates that the activation rate of the omeprazole correlates with the pH in the cells, therefore, it is possible under *in vivo* conditions acidification was not sufficient to inhibit the gill H^+/K^+-ATPase since the pH was not adjusted during the experiments. In future studies, the *in vitro* measurements of H^+/K^+-ATPase activity from the organs of treated fish would address this question of effective pump inhibition. It is also possible that the omeprazole was cleared since in mammalian studies, omeprazole is rapidly cleared from the plasma with a half-life of less than one hour through metabolized by the liver (Larson et al. 1985).

As mentioned above, the kinetics of the accumulation of Rb^+ over time suggested the presence of carrier mediated uptake of Rb^+. This promising observation led me to look for further pharmacological evidence of HKA using a different methodology, an *ex vivo* preparation. With this preparation I had more control over the tissue and the experimental surroundings including the pH which is known to be an essential factor for the activation and binding of the proton pump inhibitors.

4.2 *Ex vivo Preparation*

My *ex vivo* results along with the Rb^+ uptake results in the *in vivo* experiment, support the hypothesis that the gastric type H^+/K^+-ATPase plays a role in K^+ and possibly acid-base regulation in *O. niloticus*. This is the first evidence of the presence of the H^+/K^+-ATPase in teleost gills and kidney. I then used omeprazole and SCH28080 as specific inhibitors for the gastric H^+/K^+-ATPase, aimed at reducing the Rb^+ uptake demonstrating the presence of the gastric H^+/K^+-ATPase in the gills and kidney. Gumz et al. (2010), in their review, reported that the gastric H^+/K^+-ATPase in tetrapod kidney is inhibited by SCH28080 and it is sensitive to omeprazole, which is supported by my results showing an inhibition in Rb^+ uptake with theses inhibitors in both kidney and gill over time.

This type of *ex vivo* approach was developed and validated by Tipsmark and Madsen (2001) in gills and kidney of salmonid fish with the inhibitor ouabain to study the Na^+/K^+-ATPase. Since I was studying a different pump (H^+/K^+-ATPase) that is sensitive to different inhibitors (omeprazole and SCH28080), some modifications were done to the approach to fit the experiments. As expected gill and kidney inhibition rates were significantly noticeable within 10 min of the start of the experiment, demonstrating that the inhibitors were blocking the uptake of Rb^+ and reducing the pump activity as time increased. Although, inhibition with SCH28080 was only tested on gill at 10 min, it shows a high degree of inhibition (50%). Gumz et al. (2010) reviewed that the gastric H^+/K^+-ATPase in tetrapod kidney is inhibited by SCH28080 and it is sensitive to omeprazole, which is supported by my results.

As described by Tipsmark and Madsen (2001) studying NKA, I also pre-incubated tissues in Rb^+ ringer solution before adding the inhibitors (omeprazole and SCH28080). This resulted in

a significant inhibition of the Rb^+ uptake rate by about 50% for the experimented time course. However, I believe that, higher inhibition rates would have occurred if some changes in the approach were done. For example pre-incubating the tissue with inhibitor first and then supply it with Rb^+ ringer solution, which is evident from the decrease in Rb^+ uptake overtime with omeprazole treatment.. These refinements should be tested in future studies.

A potential challenge with all *ex vivo* preparations is tissue degradation. Although the tissues were capable of take up of Rb^+ over 30 min further compelling evidence for tissue integrity was provided by the LDH activity measurements. I used LDH as the most common marker to measure the leakage rate of this cytosolic enzymes into the medium, as an indicator of cell damage and death. The resultant average leakage rate out of the tissue was extremely low about (0.03%) through experimental acclimations but with no time or treatment dependent correlations. However, the only point when the tissue gills shows a leakage rates higher than the average was at time 0h, yet this was reasonable since all excised tissue were cut in one plate which might leak some of the enzyme while cutting, then the tissue was moved to the 24-well plate where it was thoroughly rinsed (see LDH assay). Tissues meant for time zero were assayed immediately after a couple of rinses, therefore, those tissues had a slightly higher leakage rate (0.1%) due to the slight rinsing in comparison to the amount of enzyme residue they were exposed to. However, these activity levels were still very low indicating the maintenance of tissue integrity during the course of the experiment and significantly no correlation with inhibitor treatments. In comparable studies that measure LDH activity levels in U/g wet mass tissue, the same range of values are reported in *Mugil auratus* (81 U/g Krajnovic-Ozretic and Ozretic 1987) and *Fundulus heteroclitus* (51.8 U/g; Diaz 2014).

4.3 Immunolocalization

My results are the first to demonstrate that a gastric H^+/K^+-ATPase in a freshwater teleost is expressed in extragastric sites where it may function in K^+ absorption. Choe et al. (2004) were the first to detect an initial expression of HKα1 (Atp4a) in the gills of a freshwater elasmobranch (*D.sabina*), and Hentschel *et al.* (1993) in the kidney of a marine elasmobranch (*Scyliorhinus caniculus*) suggesting that the HKα1 isoform of elasmobranch is similar of that in rat gastric parietal cells and renal intercalated cells, with 81.4% similarlity to the rat HKα1 protein sE quench. Smolka et al. (1984) had already confirmed the crossreactivity of the antibodies used in these studies with those proteins found in the gastric glands. While all the type IIc P-ATPases share homology, *D.sabina* alignment with *O.niloticus* Atp4a isoform from GenBank shows that the *O.niloticus* protein shares similarities in many regions, including the invariant phosphorylation site and the predicted transmembrane regions of type HKα1. Furthermore, the *O.niloticus* sequence is 86% identical to *D.sabina*.

Nile tilapia (*O. niloticus*) stomach was shown to be immunoreactive to antibodies generated against Atp4a and Atp4b indicating that they recognize the *O. niloticus* gastric proton pump. My results in gills indicate that gastric H^+/K^+-ATPase immunoreactivity occurred apically in a subpopulation of mitochondrion-rich chloride cells or ionocytes. This cell type with its subtypes is distributed in teleost fish gills and is the site of ion uptake (Wilson & Laurent, 2002; Dymowska et al., 2012), although, the subtypes that are responsible for K^+ uptake had not been identified until my work.

Knowing that both H^+/K^+-ATPase isoforms are localized to the colleting duct of mammalian kidney, just as in mammals my gastric H^+/K^+-ATPase immunoreactivity was also

found in the collecting duct of *O.niloticus* thus emphasizing its role in K^+ reabsorption and possibly acid base balance. As this segment has the ability to acidify the tubular fluid by secreting H^+ and reabsorb K^+ thus playing a role in acid-base and potassium regulation in tetrapod (Koeppen, 2009; Gumz et al., 2010). In the kidney of a marine elasmobranch (*Scyliorhinus caniculus*), gastric H^+/K^+-ATPase immunoreactivity was found in the late distal tubule as well as the proximal tubule (Hentschel et al., 1993).

4.4 Potassium regulation

The main finding of my thesis is that tilapia can take up potassium and that the HKA is involved. Potassium regulation is important to animals. Animals and humans obtain potassium through food at levels that does not pose health risks, however, minor disturbances (increase - decrease) in potassium concentration might cause serious health risks. In mammals for example, unfavorable effects might occur when they are subjected to higher than normal K^+ plasma concentrations greater than 5.0 mmol/L (hyperkalemia), or when K^+ plasma concentrations are lower (hypokalemia) than the normal range (3.5–5.0 mmol/L). Both hyperkalemia and hypokalemia result from disruptions in transcellular homeostasis or in the renal regulation of K^+ excretion (Talling, 2010). However, since a normal kidney can excrete hundreds of mEq of K^+ daily, excessive K^+ intake is an uncommon cause of hyperkalemia without other contributing factors. Therefore, if renal K^+ excretion is impaired, whether through drugs, renal insufficiency, or other causes, then excess K^+ intake can produce hyperkalemia,. On the other hand, , K^+ depletion (hypokalemia) by the kidney is commonly caused by polyuria (higher rates of urination) and polydipsia (excessive thirst) which can lead to excessive drinking and dilution of K^+ in the blood. Sustained K^+ depletion can severely affect systems and organs leading to cluding cardiovascular

and neurological disturbances and impaired muscle and kidney function. In aquatic animals maintenance of potassium homeostasis is vital as well. Although little work has been done in fishes, it would be predicted that strenuous exercise and a diet and environment (e.g. fresh water) poor in K^+ would result in hypokalemia whereas diets and environments (e.g. sea water) rich in K^+ would be predicted to result in hyperkalemia if regulatory mechanisms were impaired.

There are specific membrane enzymes (ATPases) or transporters that manage the interrelations between internal and external concentrations that are governed by a two-way dynamic exchange, powered by ATP hydrolysis. This mechanism was proposed by (Shin, et.al., 2009) and supported by (Talling, 2010) with both focused on the enzymes required to transfer K^+ in order to maintain K^+ balance. This included the Na^+/K^+-ATPase, which actively pumps K^+ in and Na^+ out of the cell in a 2:3 ratio and is responsible for generating the resting membrane potential. Another enzyme, the H^+/K^+-ATPase, which is the central focus of my thesis, transports the hydronium ion in exchange for potassium ion with stoichiometry changing with the pH gradient; $2H^+$: $2K^+$: 1ATP at neutral pH to $1H^+$: $1K^+$: 1ATP at pH < 3.

4.5 The model for K^+ uptake

Based on my findings of an apical localization of the HKA in gill ionocytes and kidney collecting duct, I predict the following model to explain HKA's role in K^+ uptake in Figure 4.1. The HKA uses the energy from ATP hydrolysis to power the electroneutral exchange of intracellular H^+ for extracellular K^+ (Caplan 1998). The uptake K^+ would be against its electrochemical gradient. Intracellular K^+ would exit the cell down its electrochemical gradient across the basolateral membrane via an inwardly rectifying K^+ channel (Evans et al. 2005). My IHC results show that these cells are also rich in basolateral NKA however it role in K^+ uptake is likely an indirect and/or

related to driving other transport processes. It should be noted that K^+ is but one of many ions that may be transported by gill ionocytes for ion and acid-base regulation (Evans et al. 2005).

4.6 Conclusions

In summary, this research was the first to demonstrate the expression and role of the gastric proton pump H^+/K^+-ATPase as an extra gastric pump outside the stomach (gill and kidney) in a teleost species. Evidence included omeprazole- and SCH28080-induced inhibition of the gastric proton pump in teleost (*O.niloticus*) gills and kidney suggesting a role in K^+ reabsorption and possibly acid base regulation..Immunohistochemistry demonstrated that the pump was localized apically in the gill ionocyte and the kidney collecting duct segment. In the future, it is vital to better understand the HKA's role through *ex vivo* and *in vivo* experiments and testing in different teleost species to determine how wide spread, and what role the H^+/K^+-ATPase, plays in teleost physiology. Of particular interest, will be determining what role the pump plays in in acid-base regulation. .

5. Lay summary:

In aquatic environments fishes face many challenges,, including the need to maintain ion and acid base balance between the internal and external environments. The most vital ions that need to be regulated are Na^+ and Cl^-, as well as potassium. Even small disturbances in K^+ concentrations can interfere with nervous system and muscle function. The mechanism that helps to maintain K^+ balance is mediated by the H^+/ K^+-ATPase (HKA), using the energy from the hydrolysis of ATP to transport H^+ and K^+ ions against their concentration gradients. There are two different types of H^+/ K^+-ATPase; the gastric HKA and the non-gastric HKA (not found in *O. niloticus*). The gastric H^+/ K^+-ATPase consists of HKα1 (Atp4a) and β (Atp4b) subunits. It is well known that this pump is expressed in the mammalian stomach and kidney playing a role in producing the gastric acid

(HCl) and acidifying the stomach content, and contributing to efficient renal K^+ retention. Since gills have many of the functions of kidney in mammals and are the site of active K^+ absorption, I suggest that this pump is expressed in the teleost fish as an extra gastric H^+/ K^+-ATPase with a role in ion and acid base regulation. By measuring Rb^+ uptake from the water as a surrogate for K^+, I was able to demonstrate that the tilapia takes up K^+. The uptake of Rb^+ was also inhibited using the drug omeprazole and SCH28080,, which are stomach ulcer drugs that block the action of the H^+/K^+ pump. Immunohistochemistry was used to localize the gastric H^+/ K^+-ATPase (both α and β subunits) in the gill. The H^+/ K^+-ATPase was located apically in the gill's ionocytes and kidney's collecting duct segment suggesting a role in K^+ reabsorption and possibly acid base regulation. To conclude, my thesis provided the first evidence of the function, expression, and role of the extra gastric H^+/ K^+-ATPase in a teleost fish (*O. niloticus*).

6. Integrative aspect of thesis

Since various organs and systems combine to effectively accomplish the regulation of whole animal homeostasis through cellular processes, such as energy production, membrane transport, cellular anatomy and gene expression, this research has integrated molecular, biochemical, cellular and whole animal techniques. Notably knowing how cells work is essential to understand complex physiological processes in the whole organism. Also, to appreciate the homeostatic mechanisms at play in potassium and acid-base regulation, it is necessary to integrate our understanding of the environment and phylogeny of the organism being studied.

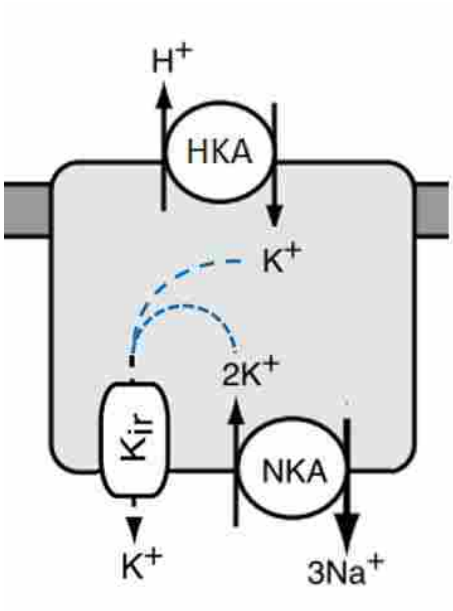

Figure 4.1 Summary of gill/kidney HKA in *O. niloticus*. HKA is found apically in both gill ionocytes and kidney distal tubule. ATP hydrolysis by the NKA drives electroneutral hydrogen and potassium exchange. The accumulated intracellular K^+ exits the cell across the basolateral membrane down its electrochemical gradient via an inwardly rectifying potassium channel (Kir). The basolateral NKA Figure modified from Evans et al. (2005).

6. References:

Burry, R. W. (2011). Controls for immunocytochemistry: an update. *The Journal of Histochemistry and Cytochemistry : Official Journal of the Histochemistry Society*, *59*(1), 6–12. http://doi.org/10.1369/jhc.2010.956920

Caplan, M. J. (1998). Gastric H^+ / K^+ -ATPase : targeting signals in the regulation of physiologic function. *Current Opinion in Cell Biology*,10: 468–473. http://doi.org/10.1016/S0955-0674(98)80060-4

Choe, K. P., Verlander, J. W., Wingo, C. S., & Evans, D. H. (2004). A putative H^+-K^+-ATPase in the Atlantic stingray, *Dasyatis sabina*: primary sequence and expression in gills. *American Journal of Physiology. Regulatory, Integrative and Comparative Physiology*, *287*(4), R981–R991. http://doi.org/10.1152/ajpregu.00513.2003

Codina, J., & DuBose, T. D. (2006). Molecular regulation and physiology of the H^+,K^+ -ATPases in kidney. *Seminars in Nephrology*, *26*(5), 345–51. http://doi.org/10.1016/j.semnephrol.2006.07.003

Dennis Brown, Richard Bouley, and H. A. J. L. (1998). New insights into the dynamic regulation of water and acid-base balance by renal epithelial cells. *Nephrology Nursing Journal : Journal of the American Nephrology Nurses' Association*, *31*(2), 201-6-8.

Dymowska, A. K., Hwang, P. P., & Goss, G. G. (2012). Structure and function of ionocytes in the freshwater fish gill. *Respiratory Physiology and Neurobiology*, *184*(3), 282–292. http://doi.org/10.1016/j.resp.2012.08.025

Eddy, F. B. (1985). Uptake and loss of potassium by rainbow trout (*Salmo gairdneri*) in fresh

water and dilute sea water. *Journal of Experimental Biology*, *118*(1), 277–286.

Edwards, S. L., Donald, J. A., Toop, T., Donowitz, M., & Tse, C. (2002). Immunolocalisation of sodium proton exchanger like proteins in the gills of elasmobranchs. *Comparative Biochemistry and Physiology* 131A, 257–265.

Ekberg, K., Pedersen, B. P., Sorensen, D. M., Nielsen, A. K., Veierskov, B., & Nissen, P. (2010). Structural identification of cation binding pockets in the plasma membrane proton pump. *Proceedings of the National Academy of Sciences*, *107*,.21400-21405. http://doi.org/10.1073/pnas.1010416107/-/DCSupplemental.www.pnas.org/cgi/doi/10.1073/pnas.1010416107

Evans, D. H. (2002). Acid-base regulation in fishes: Cellular and molecular mechanisms. *Journal of Experimental Zoology*, *293*(3), 302–319. http://doi.org/10.1002/jez.10125

Evans, D. H., Piermarini, P. M., & Choe, K. P. (2005). The Multifunctional Fish Gill : Dominant Site of Gas Exchange , Osmoregulation , Acid-Base Regulation , and Excretion of Nitrogenous Waste. *Physiological Reviews*, *85*, 97–177. http://doi.org/10.1152/physrev.00050.2003.

Goss, G. G., Perry, S. F., Fryer, J. N., & Laurent, P. (1998). Gill morphology and acid-base regulation in freshwater fishes. *Comparative Biochemistry and Physiology - A Molecular and Integrative Physiology*, *119*(1), 107–115. http://doi.org/10.1016/S1095-6433(97)00401-7

Gumz, M. L., Lynch, I. J., Greenlee, M. M., Cain, B. D., Wingo, C. S., (2010). The renal H^+ -K^+ -ATPases : physiology , regulation , and structure. *American Journal of Physiology 298*(1), F12-F21. http://doi.org/10.1152/ajprenal.90723.2008

Harlow, E., & Lane, D. (1988). Antibodies: A Laboratory Manual, 726.

Health Canada. (2008). Guidance on Potassium from Water Softeners. Water, Air and Climate Change Bureau, Healthy Environments and Consumer Safety Branch, Health Canada, Ottawa, Ontario, 21.

Henry, R. P., Lucu, Č., Onken, H., & Weihrauch, D. (2012). Multiple functions of the crustacean gill: osmotic/ionic regulation, acid-base balance, ammonia excretion, and bioaccumulation of toxic metals. *Frontiers in Physiology*, *3*, 1–33. http://doi.org/10.3389/fphys.2012.00431

Hersey, S. J., Steiner, L., Mendlein, J., Rabon, E., & G.Sachs. (1988). SCH28080 prevents omeprazole inhibition of the gastric H^+ / K^+-ATPase. *Biochimica et Biophysica Acta (BBA)-Protein Structure and Molecular Enzymology*, *956*(1), 49-57.

Hwang, P.-P., Lee, T.-H., & Lin, L.-Y. (2011). Ion regulation in fish gills: recent progress in the cellular and molecular mechanisms. *American Journal of Physiology. Regulatory, Integrative and Comparative Physiology*, *301*(1), R28–R47. http://doi.org/10.1152/ajpregu.00047.2011

Shin, J.M and Sachs, G. (2010). Pharmacology of proton pump inhibitors, *Current Gastroenterology Reports 10*(6), 528–534.

Koeppen, B. M. (2009). The kidney and acid-base regulation. *Advances in Physiology Education*, *33*(4), 275–281. http://doi.org/10.1152/advan.00054.2009

Larsson, H., H. Mattson, G. Sundell, and E. Carlsson. (1985). Animal pharmacodynamics of omeprazole. A survey of its pharmacological properties in vivo. *Scandinavian Journal of Gastroenterology. Supplement 108*, 23-35.

Lin, H., and Randall, D. (1991). Evidence for the presence of an electrogenic proton pump on the trout gill epithelium, *Journal of Experimental Biology 161*, 119–134.

Lin, C.-H., Shih, T.-H., Liu, S.-T., Hsu, H.-H., & Hwang, P.-P. (2015). Cortisol regulates acid secretion of h+-atpase-rich ionocytes in zebrafish (*Danio rerio*) embryos. *Frontiers in Physiology*, *6*, 1–11. http://doi.org/10.3389/fphys.2015.00328

Liquori, G. E., Zizza, S., Mastrodonato, M., Scillitani, G., Calamita, G., and Ferri, D. (2005). Pepsinogen and H,K-ATPase mediate acid secretion in gastric glands of *Triturus carnifex* (Amphibia, Caudata). *Acta Histochemica*, *107*(2), 133–41. http://doi.org/10.1016/j.acthis.2005.03.002

Maclean, N., Rahman, M. a., Sohm, F., Hwang, G., Iyengar, A., Ayad, H., and Farahmand, H. (2002). Transgenic tilapia and the tilapia genome. *Gene*, *295*(2), 265–277. http://doi.org/10.1016/S0378-1119(02)00735-7

Marshall, W. S., & Grosell, M. (2005). Ion Osmoregulation , and Acid – Base Balance. *The Physiology of Fishes* (Eds Evans D.H, Claiborne J.D.) CRC Press Boca Raton. pp177–230.

Pedersen, P.L., Carafoli, E. (1987) Ion motive ATPases. I. Ubiquity, properties, and significance to cell function. *Trends in Biochemical Sciences*. 12:146-50.

Perry, S. F., & Gilmour, K. M. (2006). Acid-base balance and CO2 excretion in fish: Unanswered questions and emerging models. *Respiratory Physiology and Neurobiology*, *154*(1–2), 199–215. http://doi.org/10.1016/j.resp.2006.04.010

Perry, S. F., Shahsavarani, A., Georgalis, T., Bayaa, M., Furimsky, M., & Thomas, S. L. Y. (2003). Channels, pumps, and exchangers in the gill and kidney of freshwater fishes: their

role in ionic and acid-base regulation. *Journal of Experimental Zoology. Part A, 300*(1), 53–62. http://doi.org/10.1002/jez.a.10309

Shin, J. M., Munson, K., Vagin, O., & Sachs, G. (2009). The gastric HK-ATPase: Structure, function, and inhibition. *Pflugers Archiv European Journal of Physiology*, *457*(3), 609–622. http://doi.org/10.1007/s00424-008-0495-4

Singh, V., Mani, I., & Chaudhary, D. K. (2013). ATP4A gene regulatory network for fine-tuning of proton pump and ion channels. *Systems and Synthetic Biology*, *7*(1–2), 23–32. http://doi.org/10.1007/s11693-012-9103-1

Dietz, T.H. and R. A. Byrne. (1990). Potassium and rubidium uptake in freshwater bivalves, *Journal of Experimental Biology 405*, 395–405.

Talling, A. J. F. (2010). Potassium — A Non-Limiting Nutrient in Fresh Waters ? Potassium – a non-limiting nutrient in fresh waters ? *Freshwater Reviews*, *3*(2), 97–104. http://doi.org/10.1608/FRJ-3.2.1

Weiner, I. D. and Wingo, C. S. (1998). Hyperkalemia: a Potencial Silent Killer. *Journal of the American Society of Nephrology*, *9*, 1535–1543.

Welling, P. A. (2013). Regulation of renal potassium secretion: Molecular mechanisms. *Seminars in Nephrology*, *33*, 215–228. http://doi.org/10.1016/j.semnephrol.2013.04.002

Wilcox, S. J., & Dietz, T. H. (1995). Potassium transport in the freshwater bivalve *Dreissena polymorpha*, *Journal of experimental biology*, *198*, 861–868.

Wilson, J. M. (2011). Morphology of Branchial Ionocytes. *Encyclopedia of Fish Physiology* (Vol. 2). Elsevier Inc. http://doi.org/10.1016/B978-0-12-374553-8.00202-1

Wilson, J. M., & Castro, L. F. C. (2010). Morphological diversity of the gastrointestinal tract in fishes, Fish Physiology *30*(10), 1–55. http://doi.org/10.1016/S1546-5098(10)03001-3

Wilson, J. M., and Laurent, P. (2002). Fish gill morphology: Inside out. *Journal of Experimental Zoology*, *293*(3), 192–213. http://doi.org/10.1002/jez.10124

Wingo, C. S., and Cain, B. D. (1993). The renal H-K-ATPase : Physiological Significance and Role in Potassium Homeostasis. *Annual Review of Physiology*, *55*, 47–323.

Worden, J.C. and Hanna, K.S. (2017). Optimizing proton pump inhibitor therapy for treatment of nonvariceal upper gastrointestinal bleeding. *American Journal of Health-System Pharmacy*, *74*(3), 109-116.